Journal Pre-proof

Regional haze formation enhanced the atmospheric pollution levels in the Yangtze River Delta region, China: Implications for anthropogenic sources and secondary aerosol formation

Mozammel Haque, Cao Fang, Jürgen Schnelle-Kreis, Gülcin Abbaszade, Xiaoyan Liu, Mengying Bao, Wenqi Zhang, Yan-Lin Zhang

Please cite this article as: M. Haque, C. Fang, J. Schnelle-Kreis, et al., Regional haze formation enhanced the atmospheric pollution levels in the Yangtze River Delta region, China: Implications for anthropogenic sources and secondary aerosol formation, *Science of the Total Environment* (2020), https://doi.org/10.1016/j.scitotenv.2020.138013

This is a PDF file of an article that has undergone enhancements after acceptance, such as the addition of a cover page and metadata, and formatting for readability, but it is not yet the definitive version of record. This version will undergo additional copyediting, typesetting and review before it is published in its final form, but we are providing this version to give early visibility of the article. Please note that, during the production process, errors may be discovered which could affect the content, and all legal disclaimers that apply to the journal pertain.

Regional haze formation enhanced the atmospheric pollution levels in the Yangtze River Delta region, China: implications for anthropogenic sources and secondary aerosol formation

Md. Mozammel Haque[1,2,3], Cao Fang[1,3], Jürgen Schnelle-Kreis[4], Gülcin Abbaszade[5], Xiaoyan Liu[1,3], Mengying Bao[1,3], Wenqi Zhang[1,3], and Yan-Lin Zhang[1,3]

[1]*Yale-NUIST Center on Atmospheric Environment, International Joint Laboratory on Climate and Environment Change (ILCEC), Nanjing University of Information Science & Technology, Nanjing 210044, China*
[2]*State Key Laboratory of Organic Geochemistry, Guangzhou Institute of Geochemistry, Chinese Academy of Sciences, Guangzhou 510640, China*
[3]*Jiangsu Provincial Key Laboratory of Agricultural Meteorology, School of Applied Meteorology, Nanjing University of Information Science & Technology, Nanjing 210044, China*
[4]*Helmholtz Zentrum Munchen, Joint Mass Spectrometry Ctr, Cooperat Grp Comprehens Mol Analyt, D-85764 Neuherberg, Germany*
[5]*Helmholtz Zentrum Munchen, Joint Mass Spectrometry Ctr, Cooperat Grp Comprehens Mol Analyt CMA,Gmunder Str 37, D-81479 Munich, Germany*

Corresponding author
Yan-Lin Zhang
E-mail: dryanlinzhang@outlook.com

16 March, 2020

Abstract

High-time-resolution (3-hour) $PM_{2.5}$ samples were collected simultaneously from the rural and urban areas in the Yangtze River Delta region during winter. The aerosol samples were analyzed for carbonaceous components, organic tracers, water-soluble inorganic ions and stable carbon ($\delta^{13}C$) and nitrogen ($\delta^{15}N$) isotopic compositions of total carbon and total nitrogen. The values of $PM_{2.5}$ and secondary organic carbon (SOC) for both sampling sites were observed 2 times higher in haze events compare to those in clear days, implying severe pollution occurred by photochemical oxidation during haze periods. The PM mass of rural samples showed similar temporal trend and significant correlation with the urban PM, reflecting pollution sources or their formation process are most likely identical. Diurnal variations of $PM_{2.5}$ and carbonaceous components revealed that pollution levels increased at daytime due to the photochemical oxidation. In addition, SOC and OC were influenced by the relative humidity (RH%) and temperature (T °C), indicating that such meteorological factors play important roles in the occurrence of regional air pollution. The concentrations of levoglucosan, polycyclic aromatic hydrocarbons, hopanes, and n-alkanes were 625±456 and 519±301 ng m^{-3}, 32.6±24.7 and 28.7±20.1 ng m^{-3}, 1.83±1.51 and 1.26±1.34 ng m^{-3}, and 302±206 and 169±131 ng m^{-3} for rural and urban samples, respectively. Levoglucosan is the most abundant organic compounds, exhibited 2-3 times higher in haze than clear days, suggesting biomass burning (BB) emission substantially affects the haze pollution in winter. Furthermore, NO_3^- was the dominant ionic species followed by SO_4^{2-}, NH_4^+, Cl^- and other minor species for both sites. The $\delta^{13}C$ and $\delta^{15}N$ values demonstrate that anthropogenic activities such as fossil fuel combustion and BB are the major sources for carbonaceous and nitrogenous aerosols. This study implies that both the regional anthropogenic emissions and meteorological conditions influenced the regional haze formation, leading enhancement of pollution levels in eastern China during winter.

1. Introduction

Atmospheric particulate matter (PM) contains various organic and inorganic species, whereas many of them can affect human health and the Earth's climate. Both natural (e.g., forest fires, soil dust, volcanic dust, sea-salt, botanical debris) and anthropogenic (e.g., open burning, fossil-fuel, vehicular emissions, and industrial processes) sources produce numerous organic and inorganic gases and particles, which are emitted into the atmosphere (IPCC, 2001). They are also derived via the atmospheric oxidation of organic and inorganic species in the presence of sunlight and oxidants. Organic aerosol (OA) is one of the major parts of PM, accounting for up to 70% of the aerosol mass (Kanakidou et al., 2005). OAs contribute to the radiative balance by scattering sunlight, control the physiochemical properties of particles and potentially influence the hygroscopic activities (Hemming and Seinfeld, 2001; Kanakidou et al., 2005). OAs play important roles in the atmosphere to change the global and regional climate, biogeochemical cycling and chemical compositions (Kanakidou et al., 2005; P̈oschl, 2005). It is essential to fully understand the sources and molecular composition of OA for better evaluation of their potential impacts. Molecular markers are usually used to assess source contributions of aerosols whether it is dominated by primary or secondary organic carbon (Sheesley et al., 2015). Inorganic components in atmospheric aerosols are also a great concern for their climatic effect. They are more water-soluble and their hygroscopic properties are much higher than organics, resulting in the enhancement of CCN activity of particles (Zhang et al., 2012a). Biomass burning (BB) and fossil fuel combustions produce a large amount of organic and inorganic aerosols, which contribute widely to the global atmospheric particles (Bond et al., 2004; Huang et al., 2014).

Many types of trace gases, organic and inorganic species are produced during BB activities. On a global scale, BB is the largest source of primary carbonaceous aerosols in the atmosphere (Bond et al., 2004; Andreae and Merlet, 2001; Forster et al., 2007; Guenther et

al., 2006). The pollutants originated from BB can be transported long distances downwind from the source areas. BB which is associated with open fires, crop residues, domestic and forest fires has drawn great scientific concern for its effects on global climate, visibility and human health (Cheng et al., 2013). Reid et al. (2005a, b) pointed out that BB particles have physical and optical properties that can affect air quality. The primary BB aerosol can be further oxidized (i.e., aging) to form a wide range of secondary organic aerosol (SOA) (Cheng et al., 2013) and secondary inorganic aerosol (SIA) (Fu et al., 2016a) during atmospheric transport. Recent studies focus on the precursors and formation mechanism of SOA from BB (Lee et al., 2008; Sun et al., 2010; Adler et al., 2011). Levoglucosan is a widely used organic molecular marker for BB which is produced by the pyrolysis of cellulose and hemicellulose in the atmosphere (Simoneit et al., 2002). Levoglucosan is considered as relatively stable in the atmosphere for several days (Fraser and Lakshmanan, 2000). However, recent studies proposed that it can be oxidized by the exposure to high loading of OH radicals during long-range transport (Zhu et al., 2015).

Fossil fuel combustion also is an important source of gases and PM in the atmosphere (Andreae and Merlet, 2001; Kan et al., 2007; Jones et al., 2009). The consumption of fossil fuel combustion has been increased for the last decades due to the high urbanization rate with industrial development, vehicular traffic, and population growth (Bourotte et al., 2005). Recent studies reported that coal combustion emissions have a severe effect on visibility (Chen et al., 2015) and climate change (Kim et al., 2015). Polycyclic aromatic hydrocarbons (PAHs), hopanes and n-alkanes are originated from incomplete combustion of coal, diesel, gasoline, and oil, etc. Homologs of hopanes are very stable in the atmosphere (Ding et al., 2009) which is a good indicator of vehicular emissions (Cass, 1998; Schauer et al., 1996). PAHs have adverse health effects, e.g., carcinogenicity, immunotoxicity, reproductive toxicity and genotoxicity (Sverdrup et al., 2002). PAHs are emitted from both sources of

fossil fuel combustion and BB which can be further photo-oxidized to form SOA. Low molecular weight (2 and 3 aromatic rings) PAHs are often found in the gas phase while the larger ones (4-6 aromatic rings) are observed in the particles phase (Bourotte et al., 2005). Substantial SIA precursors such as SO_2, NO_x are also emitted from fossil fuel combustion (Seinfeld and Pandis, 2006).

Ambient $PM_{2.5}$ pollution has occurred frequently due to the rapid industrialization and urbanization, seriously influencing human health, local air quality, regional and global climate change, led to a great concern (Shao et al., 2006; Reiss et al., 2007; Zhang et al., 2012b; Huang et al., 2014). BB, coal combustion, vehicular and industrial emissions are the major sources of heavy haze pollution in China (Adame et al., 2012; Zhang et al., 2015a; Cao et al., 2016). OAs account generally for ∼20-45% of $PM_{2.5}$ in China, which is around five times higher than that found in North America and Europe (Wu et al., 2018). Numerous studies have been conducted on the characterization of organic (Wang et al., 2006a, b, 2009a, 2011; Fu et al., 2008, 2014, Ding et al., 2014) and inorganic (Bergin et al., 2001, VanCuren and Cahill, 2002) aerosols from China. However, this is one of the first studies for simultaneous high-time-resolution (3 hrs interval) studies of OAs in urban and rural sites from China based on multiple offline measurements. Nanjing is one of the highly populated and developed cities in eastern China where several heavy industrial regions are available. Air pollution has been a critical issue in Nanjing due to its fast urbanization and industrialization. In contrast, Dongshan, a rural area which is located on the southeast bank of the Taihu Lake of Suzhou city in eastern China. Taihu Lake plain in Suzhou city is considered under the pollution transport belt which overlaps the Yangtze River Economic Belt (Chang et al., 2017). Dongshan, a receptor site, has a unique topography and humid climate where atmospheric pollutants are transported from its surrounding polluted areas. It has an eastern Asian monsoon climate with four clear seasons where prevailing winds change

seasonally. Both of the sampling sites are located in the Yangtze River Delta (YRD) region in the Jiangsu province which is under the control of long-range transport of air pollution in China. Previous field measurements, model simulations, and satellite observations studies have found that inter-province transport of air pollutants emitted from anthropogenic activities was a potential source of air pollution throughout the YRD region.

In order to understand the sources and formation of regional air pollutions, chemical compositions of organic and inorganic aerosols along with organic carbon (OC), elemental carbon (EC) as well as stable carbon and nitrogen isotopic compositions of TC and TN have been studied in $PM_{2.5}$ samples from the rural (Dongshan) and urban (Nanjing) sites in eastern China. Here, we discuss regional haze pollutions, enhanced by secondary aerosol formation when meteorological factors may influence the formation process significantly. The molecular characteristics of organic and inorganic aerosols, diurnal variations, and potential sources are also discussed.

2. Experimental

2.1 Sample collection

The aerosol sampling campaign was conducted simultaneously in rural (Dongshan) and urban sites (Nanjing) in eastern China (Fig. 1). The 3-h $PM_{2.5}$ samples were collected from the Dongshan (31.04°N, 120.26°E) and Nanjing (32.09°N, 118.78°E) using medium and high-volume sampler (Laoshan, Quingdao, China) from 15-28 January 2015. A total of 192 (96+96) samples have been collected on precombusted (450 °C, 6 h) quartz fiber filters with sizes of 80 mm at a flow rate of 100 L min^{-1} and 8 x 10 inches at a flow rate of 1.05 m^3 min^{-1} from Nanjing and Dongshan, respectively. Before and after sampling, all of the filters were equilibrated in a desiccator for 72 h with a room temperature and relative humidity at 25 ± 0.5 °C and 30 ± 5%, respectively. After being equilibrated, the filters were weighed to

determine the aerosol mass and then wrapped in aluminum foils, packed in sealable polyethylene bags and stored at -20 °C until the analysis.

2.2 Gas chromatography-mass spectrometry (GC-MS) analysis

Organic species were analyzed by in situ derivatization thermal desorption followed by gas chromatography and time-of-flight mass spectrometry (IDTD-GC-TOF-MS) (Orasche et al., 2011). Filter punches of 4-6 mm diameter were used for analysis. Filter samples were placed into a direct thermal desorption unit (Linex and Optic 3, Atas GL, Netherlands) mounted to the gas chromatograph while internal standards (isotope labelled compounds) and 10 µL methyl-trimethylsilyl-trifluoroacetamid (MSTFA, Macherey-Nagel, Germany) were added automatically by a sampling robot (PAL Focus, Atas GL, Netherlands). During thermal extraction, MSTFA vapor was continuously added to the carrier gas stream for 16 min at the rate of 4 mL min^{-1}. After thermal extraction and derivatization, the flow rate of pure carrier gas (Helium) was reduced to 0.7 mL min^{-1} with a split flow of 50 mL min^{-1}, and GC-MS run was started. Chromatographic separation was performed on a BPX5, 25 m, 0.22 mm ID, 0.25 µm film thickness capillary column (SGE, Australia) installed in an Agilent 6890 gas chromatograph (Agilent, USA). Mass spectrometric detection (range of 35 to 500 m/z) was conducted in a Pegasus III TOF-MS (Leco, USA) using an acquisition frequency of 25 spectra per second. Evaluation of mass spectra was attempted with the Chroma TOF software package (LECO, USA). Quantification was carried out using a set of isotope labelled internal standards and external standard mixtures to acquire the individual response factors. The recovery experiment was performed three times and obtained an average value of more than 90% for organic compounds. The field-blank filters (n = 5) were analyzed following the same procedures as described above. The target compounds were not found in the blank filters. The analytical errors based on replicate analyses (n = 5) were calculated <

15 %. Details of the chemical analysis are described elsewhere (Sklorz et al., 2007; Orasche, et al., 2011).

2.3 Ion chromatography analysis

A small punch of each filter sample (5.07 cm^2) was extracted with 10.0 mL ultrapure water (> 18.2 Ω) with ultrasonication for 30 min. The extract solution was filtered to remove insoluble parts and then used for major ions analysis using ion chromatography on a ThermoFisher Scientific ICS-5000+ system (US) equipped with an automated sampler (AS-DV), a conductivity detector/chromatography compartment (DC) and a gradient pump (SP). For cation measurement, an analytical column of IonPac CS12A and a guard column of IonPac CG12A with aqueous methanesulfonic acid (MSA, 30 mM L^{-1}) eluent at a flow rate of 1 mL min^{-1}. On the contrary, anions were separated on an IonPac AS11-HC analytical column and an IonPac AG11-HC guard column with an eluent of sodium hydroxide (NaOH) gradient solution at a flow rate of 1.5 mL min^{-1} for 0-3 min, 0.5 mM L^{-1} for 3-5 min, 0.5-5 mM L^{-1} for 5-15 min, and 5-30 mM L^{-1} for 15-20 min. The volume of Loop was 200 μL. The concentrations of major ions reported here are corrected by the mean value of two field blanks.

2.4 Sample analysis for carbon fractions

OC and EC were analyzed using a Desert Research Institute (DRI) Model 2001 Thermal Optical Carbon Analyzer (Atmoslytic Inc., Calabasas, USA). An aliquot of filter sample (0.53 cm^2) was analyzed following the IMPROVE thermal optical reflectance (TOR) protocol and detailed procedures were given elsewhere (Bao et al., 2017). Furthermore, a portion of each filter (4.02 cm^2) was extracted with 10 mL ultrapure water with ultrasonication for 30 min. The water extracts were then filtered through syringe filters (0.22 μm, ANPEL, Shanghai, China) for water-soluble organic carbon (WSOC) analysis by a TOC analyzer (TOC-L, Shimadzu, Kyoto, Japan). All the concentrations of carbonaceous

components were corrected by field blanks. The analytical errors in the duplicate analyses were <5% for all carbonaceous components.

2.5 Stable isotopic compositions of TC and TN

TC and TN contents and their isotopic compositions were analyzed using element analyzer- isotope ratio mass spectrometer (EA-IRMS) (Thermo Fisher Scientific, Bremen, Germany). A punch (1.53 cm^2) of each filter sample was cut off and put into a tin cup. The tin cups were shaped into rounded balls using a pair of flat-tipped tweezers and put into the autosampler of EA. The tin cups were rounded using a pair of flat-tipped tweezers and placed into the autosampler of EA to analyze TC/TN and their isotopic ratios. The detailed procedures were reported elsewhere (Fan et al., 2019; Zhang et al., 2019). Isotope data reported as δ^{13}C and δ^{15}N values were defined as (Wang et al., 2017):

$$\delta\ ^{13}C\ (‰) = [(^{13}C/^{12}C)_{sample} / (^{13}C/^{12}C)_{standard}-1] \times 1000 \qquad (1)$$

$$\delta\ ^{15}N\ (‰) = [(^{15}N/^{14}N)_{sample} / (^{15}N/^{14}N)_{standard}-1] \times 1000 \qquad (2)$$

δ ^{13}C and δ ^{15}N values reported here were corrected by field blanks.

3. Results and discussion

3.1 Meteorological effects and diurnal variations

Both sampling sites are located in Jiangsu province in the eastern part of China, whereas distance is around 200 km between them. Mostly similar temporal trends were observed for meteorological parameters for both sampling areas (Fig. 2). However, wind speed (WS) and relative humidity (RH%) were higher in the rural area (WS; 2.46 m s^{-1} and RH; 74%) than those in urban area (WS; 0.99 m s^{-1} and RH; 61%) due to the location of this rural site nearby lake area. The average temperature and visibility were 6.8 °C and 4.1 Km for rural as well as 6.2 °C and 3.2 Km for urban sites, respectively. Two severe haze periods (2015.01.16, 10:00-2015.01.17, 4:00 and 2015.01.21, 4:00-2015.01.28, 6:00) were observed during the campaign when visibility was mostly less than 3 Km with higher RH (Fig. 2). One

9

dust event was also found from 2015.01.18, 10:00 to 2015.01.24, 22:00 when Ca^{2+} concentrations were high which is discussed in section 3.4. The prevailing winds in Dongshan are originated from the south- and northwest during the winter period when some air masses pass over Nanjing.

Figure 3 shows the temperature (T) and RH-dependent distributions of OC, EC, and SOC mass concentrations throughout the sampling period. OC showed a strong dependency on RH and T in rural samples when the highest mass loading observed with high RH and T, indicating a major part of OC associated with secondary formation at the rural area as primary OC should not be influenced by those factors. In contrast, urban OC found to be less influenced by RH and T compare to rural samples, implying complex sources of OC in the urban area. Chang et al. (2017) reported complicated sources of OC in Shanghai city. Loadings of EC for both sampling sites are not clearly dependent on RH and T which is reasonable because EC is a primary emission particle. However, SOC for both sampling sites was highly RH- and T-dependent when the highest mass loading (>30 μg m^{-3} for rural and >20 μg m^{-3} for urban) documented at RH >50% and T >8 °C. These results reveal that SOA formation occurred by aqueous phase and photochemical oxidation reactions in the YRD regions during winter.

Diurnal variations of PM mass, carbonaceous components, organic compounds, and major ions concentrations are shown in Figs. 4 and 5. The higher values (mean) of PM$_{2.5}$ were observed at daytime (10:00-13:00, 13:00-16:00 and 16:00-19:00 LT) for both sampling sites with higher 95th percentile values (Fig. 4a-b) when boundary layer heights (BLHs) were high (Rural, 509-805 m and Urban, 392-897 m), indicating secondary photochemical oxidation or more primary emissions enhanced pollution levels during daytime. It can be noted that significant values of PM$_{2.5}$ were observed at midnight to late night in urban samples which can be elucidated by an additional emission from traffic particularly heavy

diesel trucks that are only permitted to run at nighttime in the city area (Wang et al., 2007). Notably, smaller atmospheric mixing due to lower BLHs during nighttime (Rural, 159-199 m and Urban, 106-182 m) may be another reason for higher pollution levels at midnight to late night. OC with higher 95th percentile values was abundant at 10:00-13:00, 13:00-16:00 and 16:00-19:00 LT while a similar pattern was observed for SOC, which is comparable to $PM_{2.5}$ (Figs. 4c-d and 4g-h) for both sampling sites. It reflects that photochemical oxidation at daytime enhances the pollution level along with secondary aerosol formation during this study period. In contrast, EC showed different diurnal variations with OC while higher concentrations were in the morning (4:00-7:00 and 7:00-10:00 LT) and evening (7:00-22.00 LT) in the rural area. Although urban samples exhibited high values of EC from midnight to morning (1:00-10:00 LT) and afternoon (16:00-19:00 LT) (Fig. 4e-f), which is consistent with the $PM_{2.5}$ level. The diurnal variations of EC were comparable with primary tracers of levoglucosan and PAHs (Fig. 5a-d), which is reasonable because biomass and fossil fuel combustions are the major sources for all of them. Diurnal variations of isotopic compositions of carbon ($\delta^{13}C$ for TC) (Fig. 4i-j) further support photochemical aging during daytime which is discussed in section 3.6. These results suggest that secondary aerosol formation by photochemical oxidation influences the pollution levels in the YRD region during winter. The diurnal variations of organic tracers and inorganic ions will be discussed in later sections.

3.2 PM mass and carbon fractions

The $PM_{2.5}$ mass was found to be 116 µg m^{-3} and 127 µg m^{-3} in the rural and urban sites, respectively. The concentrations of $PM_{2.5}$, carbonaceous compounds, organic and inorganic components are shown in Tables 1 and 2. Higher PM mass was observed during haze period (Rural, 144 µg m^{-3} and Urban, 152 µg m^{-3}) followed by dust (Rural, 128 µg m^{-3} and Urban, 135 µg m^{-3}) and clear days (rural, 69.7 µg m^{-3} and Urban, 76.0 µg m^{-3}) (Fig. 6a-

b), indicating more pollution occurred during haze and dust events in the YRD region. The similar temporal trend and a significant correlation of PM (r = 0.60, p<0.001) between rural and urban sites suggest that their sources or particle formation process are mostly the same (Figs. 7a and 8a). Several studies have been published in the heavy haze period during winter from China when $PM_{2.5}$ level extensively influenced by regional transport (Fu et al., 2016b; Sha et al., 2019; Sun et al., 2016; Bao et al., 2017).

Carbonaceous components are a major part of $PM_{2.5}$ with high impacts on air quality, climate change, and human health. The values of OC were observed 3.48-55.0 μg m^{-3} (mean, 21.7 μg m^{-3}) and 5.03-52.3 μg m^{-3} (21.2 μg m^{-3}) at the rural and urban site, respectively. Therefore, the concentrations of EC were found to be 0.32-11.5 μg m^{-3} (2.58 μg m^{-3}) for rural and 0.56-8.91 μg m^{-3} (2.44 μg m^{-3}) for urban aerosol. Both OC and EC showed high levels in rural than urban site (Fig. 9a). The level of OC during haze (rural, 25.5 μg m^{-3} and urban, 22.2 μg m^{-3}) and dust (26.7 μg m^{-3} and 26.7 μg m^{-3}) events were 2 times higher than clear days (12.5 μg m^{-3} and 11.7 μg m^{-3}) for both sites (Table 3). Similar patterns were also observed for EC, suggesting that mass concentrations of carbonaceous aerosols increased dramatically during pollution periods. It is of interest to note that SOC was abundant in haze days compared to dust and clear days, implied more secondary aerosol formation during the haze period, a point to be discussed in section 3.5. Chang et al. (2017) proposed that carbonaceous aerosols were derived from both local emission and regional transport in the YRD region. A profound correlation between OC and EC (r = 0.71, 0.75; p<0.001) in the rural and urban samples (Fig. S1a-b) implying their similar sources for both locations. Moreover, significant correlation coefficients of OC (r = 0.60, p<0.001) and EC (r = 0.67, p<0.001) were observed between rural and urban samples (Fig. 8b-c). These results indicate that sources or formation of carbonaceous components are mostly similar in the East China region.

WSOC is an important part of atmospheric aerosols which contributes to the cloud condensation nuclei (CCN) activities. The respective values of WSOC and water-insoluble organic carbon (WIOC) were found to be 1.97-22.6 $\mu g \ m^{-3}$ (mean 10.1 $\mu g \ m^{-3}$) and 1.53-37.5 $\mu g \ m^{-3}$ (11.6 $\mu g \ m^{-3}$) in the rural samples as well as 2.31-23.2 $\mu g \ m^{-3}$ (mean 10.3 $\mu g \ m^{-3}$) and 1.77-29.1 $\mu g \ m^{-3}$ (11.0 $\mu g \ m^{-3}$) in the urban samples, respectively. WSOC showed a significant correlation with OC at the rural (r = 0.89, p < 0.001) and urban sites (r = 0.83, p<0.001) (Fig. S1c-d), suggesting that WSOC is a crucial part of OC. On the contrary, a meaningful correlation coefficient was observed between WIOC and EC (r = 0.76, p<0.001) in the rural and urban areas (Fig. S1e-f). This result reflects that a major part of WIOC is derived from primary sources. BB could produce a large amount of WSOC (Falkovich et al., 2005; Kundu et al., 2010a), when a positive correlation was found between levoglucosan and WSOC in this study (r = 0.49 in rural and 0.73 in urban, p<0.001) (Fig. S1g-h).

3.3 Concentrations of organic markers

3.3.1 Levoglucosan

A large amount of OA is derived from BB emission in the atmosphere on a regional to a global scale. Levoglucosan is a relatively stable species in the atmosphere and may persist up to 3 days in winter while transported long distances (Mochida et al., 2010; Zhu et al., 2015). The concentration of levoglucosan was found to be 51-2500 ng m^{-3} (mean, 625 ng m^{-3}) and 100-1800 ng m^{-3} (519 ng m^{-3}) at the rural and urban sites, respectively. The higher value of levoglucosan at the rural compared to urban area (Fig. 9b) implied that different source regions or local BB sources likely, house cooking/crop residue burning involved along with regional transport in rural winter aerosol. This result is consistent with the PSCF analysis when the image showed that levoglucosan significantly contributes to the rural site from the neighboring southwest region (Fig. 10). The concentrations of levoglucosan were higher than Beijing (mean 361 ng m^{-3}, Li et al., 2018) and Tianjin (mean 185 ng m^{-3}, Wang et

al., 2006b) but lower than Chongqing (mean 2519, ng m^{-3}, Wang et al., 2006b) and Xian (mean 2915, ng m^{-3}, Wang et al., 2006b).

The values of levoglucosan in this study are comparable with the autumn non-haze period; however, 7 times lower than haze aerosol caused by wheat straw burning in 2007 in Nanjing (Wang et al., 2009b). Li et al. (2017) proposed that heavy haze pollution occurred during winter due to the crop residue and domestic BB emissions in the North China Plain (NCP) region. The PSCF analysis showed the potential contribution of levoglucosan from the north and northwest part of China to the sampling site (Fig. 10), reflecting that regional BB emission significantly influences the pollution levels in this study region. Wang et al. (2018) also reported that Nanjing was dominated by northeasterly wind during the winter monsoon. However, the local source cannot be ignored as BB emission was recorded to be an important source of fine particles in the YRD region (Feng et al., 2006; Du et al., 2011). The results of this study are consistent with the western North Pacific Rim when levoglucosan was abundantly originated from open burning, domestic heating and/or cooking in northern and northeastern China in winter (Zhu et al., 2015).

Clear diurnal patterns were observed for levoglucosan at the rural and urban sites, generally characterized by a marked peak in the morning (4:00-7:00, 7:00-10:00 LT) and in the evening (16:00-19:00 LT) (Fig. 5a-b), probably due to cooking. Higher 95th percentile values of levoglucosan were found in the morning (4:00-7:00 LT), noon (10:00-13:00 LT) and evening (19:00-22:00 LT) for rural samples, while in the late morning (7:00-10:00 LT) and early evening (16:00-19:00 LT) for urban samples, reflecting that more smoke plumes passed over the sampling sites during this period. These results are variable with the cooking time in the rural area, indicating that house cooking significantly contributes to BB emission in the rural area which can also transport to the urban area. However, the dispersion of air pollution might be the reason for the low level of levoglucosan during the daytime. Biomass

14

is the major fuel (44%) used for cooking in a rural area in China (Wu et al., 2017). Wang and Kawamura (2005) pointed out that people use various bio-fuels for cooking in a rural area in Jiangsu Province. The mean values of levoglucosan were 778 ng m^{-3}, 592 ng m^{-3}, and 349 ng m^{-3} at the rural site and 633 ng m^{-3}, 527 ng m^{-3} and 238 ng m^{-3} at the urban site in the haze, dust and clear days, respectively (Fig. 6c-d). It can be noted that several high peaks of levoglucosan were also observed for both sampling sites during the dust period (Figs. 7d and 11c) and leading to poor visibility (2.2-3.3 km, Fig. 2). It is evident that BB emission extensively influenced the haze formation during winter in this study area.

3.3.2 Polycyclic aromatic hydrocarbons

PAHs are considered as toxic substances in the atmosphere which has bad effects on human health, particularly have high cancer risk (Shrivastava et al., 2017). PAHs are mainly emitted from various anthropogenic activities such as fossil fuel combustion, BB activities and open burning of plastics, etc. The concentrations of total PAHs were found to be 2.40-136 ng m^{-3} (mean 32.6 ng m^{-3}) at the rural area and 3.50-123 ng m^{-3} (28.7 ng m^{-3}) at the urban site (Table 1). PAHs showed a significant positive correlation with levoglucosan at the rural ($r = 0.49$, $p<0.001$) and urban ($r = 0.63$, $p<0.001$) (Fig. S2a-b) sites, suggesting that PAHs partially contribute from BB activities during sampling time. The values of PAHs are comparable with Huangshi City (22.6 ng m^{-3}) in central China (Hu et al., 2018) but 2 times higher than those observed in Hong Kong (14 ng m^{-3}) (Wang et al., 2006b) and 3-4 times lower than those measured in Beijing winter aerosols (92.6 ng m^{-3}) (Yu et al., 2018). Moreover, PAHs levels of this study are much higher than those reported in other places of the world such as 2.14 ng m^{-3} in Zaragoza, Spain; 3.80 ng m^{-3} in Rio de Janeiro, Brazil; 3.16 ng m^{-3} in Atlanta, USA and 2.79 ng m^{-3} in Bangi, Malaysia (Hu et al., 2018).

A distinct diurnal pattern was found for PAHs in both sampling sites, while 95th and 75th percentile values were higher in the early morning (4:00-7:00 LT) and in the afternoon

15

(16:00-19:00) at the urban site (Fig. 5c-d) due to the more traffic emission during this period. In contrast, high values were observed during 7:00-10:00 and 19:00-22:00 (LT) at the rural site might be transported from surrounding urban areas (as less pollution from traffic emission) or local coal combustions. These results are consistent with shanghai when EC was detected high at 8:00 and 16:00 from traffic emission (Chang et al., 2017). Low molecular weight (LMW) PAHs (3- and 4-rings) were abundant, contributing to 66 % and 67 % of the total identified PAHs in the rural and urban atmosphere, respectively (Fig. S3a). Fluoranthene was detected as a dominant PAH (mean, 6.20 ng m^{-3} and 6.40 ng m^{-3}) followed by Pyrene (5.50 ng m^{-3} and 4.90 ng m^{-3}) and Benzo[b,k]fluoranthene (5.10 ng m^{-3} and 4.30 ng m^{-3}) at the rural and urban atmosphere, respectively. The similar molecular distributions patterns indicate that PAHs might share a similar source or transport pathway for both sampling sites. An abundance of LMW-PAHs in this study reflects that major part of PAHs emitted from the coal-burning of house heating and cooking because LMW-PAHs could produce more due to low combustion efficiency when high molecular weight (HMW) PAHs are formed under a higher temperature condition (Wang et al., 2009a). Moreover, LMW-PAHs are easily carried over compared to HMW-PAHs from local sources and/or longer-range atmospheric transport (Syed et al., 2017).

Some PAHs are used as indicators for their specific source emissions because different combustion conditions emit different types of PAHS. Usually, different PAHs ratios are used simultaneously to re-check the results for getting fewer uncertainties. The concentration ratios of fluoranthene / (pyrene + fluoranthene) (Flu / (Pyr + Flu)), indeno(1,2,3-cd)pyrene / (indeno[1,2,3-cd]pyrene + benzo[ghi]perylene) (IndP / (IndP + BghiP)), benzo[a]anthracene / (benzo[a]anthracene + chrysene) (BaA / (BaA + Chry)) and benzo(ghi)perylene/ benzo(e)pyrene (BghiP / BeP) are indicative of different emission sources. Yunker et al. (2002) reported that ratios of Flu / (Pyr + Flu) at 0.40-0.50 and >0.50

are attributable to the petroleum combustion (liquid fossil fuel combustion) and wood or coal combustion, respectively, whereas the current study showed this ratio of 0.54 and 0.57 at the rural and urban site, consequently. Ratios of IndP / (BghiP + IndP) were observed to be 0.34 for both sampling sites, indicating emission from petroleum combustion (diesel emissions) (Yunker et al., 2002; Bi et al., 2005). Furthermore, a BaA / (BaA + Chry) ratio of >0.5 represent biomass or coal combustion and 0.20-0.35 indicates petroleum combustion source (Khan et al. 2015; Zhang et al. 2015b), whereas our study exhibited a ratio of 0.29 for rural and 0.26 for urban samples, suggesting emission of PAHs from the vehicular exhaust. The ratio of BghiP / BeP is also one of the source indicators of PAHs when 2.0 and 0.8 indicate vehicle exhaust and coal combustion, respectively (Grimmer et al., 1983; Ohura et al., 2004). In this study, the ratio of BghiP / BeP was found to be 0.82 and 0.88 in the rural and urban areas, consequently, implying that coal combustion was the important source for PAHs. Based on the ratios of PAHs in the present study, it can be proposed that PAHs were mainly emitted from coal combustions and vehicular emission; however, partly can be derived from BB emission.

3.3.3 Hopanes

Hopanes are considered as specific biomarkers of all mineral oil and coal-based fuels. They are abundantly emitted from vehicles, crude oil and engine oil (Ding et al., 2009) and coal combustion (Oros and Simoneit, 2000). $17\alpha(H)$-$21\beta(H)$-29-norhopane ($C_{29}\alpha\beta$) and $17\alpha(H)$-$21\beta(H)$-hopane ($C_{30}\alpha\beta$) are two major hopane species identified in this study, when concentrations of total hopanes ranged from 0.20-6.40 ng m^{-3} (mean 1.83 ng m^{-3}) and 0.00-7.70 ng m-3 (1.26 ng m^{-3}) at the rural and urban site, respectively. The values of hopanes in the present study are lower than in Beijing (22.0 ng m^{-3}) (Wang et al., 2006b) but higher than Augsburg, Germany (0.54 ng m-3) (Schnelle-Kreis et al., 2007). The level of hopanes was 2-5 times higher in haze days (rural, 2.24 ng m^{-3} and urban, 1.82 ng m^{-3}) and dust days (1.86 ng

m^{-3} and 0.83 ng m^{-3}) compared to clear days (0.67 ng m^{-3} and 0.45 ng m^{-3}) in this study (Table 3).

The diagnostic ratios of hopanes are used to differentiate their emission sources. The $C_{29}\alpha\beta/C_{30}\alpha\beta$ ratios of 0.59-0.66 and 0.42 indicate emissions from gasoline and diesel, respectively, whereas 0.58-2.0 is attributable from coal-burning (Rogge et al., 1993; Oros and Simoneit, 2000). The concentration ratios of $C_{29}\alpha\beta/C_{30}\alpha\beta$ was exhibited 0.48-1.87 (mean 0.88) and 0.45-1.75 (0.94) at the rural and urban site, respectively. Most of the sample's ratios including mean values were close to those in coal combustion, suggesting hopanes are predominantly emitted from coal combustion during winter. Usually, vehicle emissions are considered as the dominant source for ambient hopanes, particularly in the traffic influenced areas. However, hopanes were abundantly found from coal combustion in Augsburg, Germany during winter while summer was dominated by vehicular emission (Schnelle-Kreis et al., 2007). Wang et al. (2009a) also reported that hopanes were mainly emitted from coal combustion in winter although summer and spring patterns were different. Moreover, the ratios of hopanes/EC can also indicate the emission source of hopanes. The ratios of hopanes/EC were observed 0.91 and 1.76 ng/μg for coal combustion and vehicle emission, respectively, from the Zhujiang tunnel, China (He et al., 2008). The average ratios of hopanes/EC in this study were found to be 0.76 and 0.61 ng/μg in the rural and urban areas, respectively, implying coal combustion emission was the major part for hopanes during the sampling period.

3.3.4 *n*-Alkanes

Homologous *n*-alkanes (C_{20}-C_{33}) were detected in the aerosol samples with a maximum at C_{21} (43 ng m^{-3} at rural and 23 ng m^{-3} at the urban site) (Table 1 and Fig. S3b). The concentrations of total identified *n*-alkanes were 36-900 ng m^{-3} (mean 303 ng m^{-3}) and 34-600 ng m^{-3} (169 ng m^{-3}) at the rural and urban sites, respectively. The values of the total *n*-

alkanes are lower than Beijing urban area (mean 426 ng m^{-3}) (Kang et al., 2018) but higher than that in another Chinese mega-city, Guangzhou (103 ng m^{-3}) (Wang et al., 2016) and more than 2 magnitude higher compared to a high-latitudinal urban area in Fairbanks, Alaska (8.35 ng m^{-3}) (Boreddy et al., 2018). The C$_{max}$ (highest concentration of n-alkanes homologs) is generally used as an indicator to identify the potential source of n-alkanes. HMW n-alkanes (C$\geq$27) are usually derived primarily from higher plant waxes (Kawamura et al., 2003), whereas LMW n-alkanes (C<27) are related to the anthropogenic emissions, e.g., fossil fuel combustion including lubricating oil, BB activities (Kang et al., 2018; Schauer et al., 2001). Kang et al. (2018) reported that LMW (C$_{18}$-C$_{24}$) n-alkanes with a major peak at C$_{23}$ were dominated in Beijing urban area during winter due to a large contribution from coal combustion while other seasons, HMW n-alkanes with a peak at C$_{29}$ were abundant from biogenic sources.

The values of LMW n-alkanes accounted for 76 % of the total quantified n-alkanes for both sampling sites, indicating a substantial contribution from anthropogenic emissions. The carbon preference index (CPI; concentration ratio of odd to even carbon number n-alkanes) is also used as a diagnostic proxy to evaluate biogenic or anthropogenic emissions (Simoneit et al., 1991). Biogenic n-alkanes that originate from vascular plant waxes, show stronger odd/even carbon number predominance with a high value of CPI (>>1), whereas CPI values are close to unity (CPI~ 1) in anthropogenic sources (Kavouras et al., 1999). The molecular distributions of n-alkanes were characterized by weak odd-carbon-numbered predominance with the CPI values ranged from 0.67-1.92 (mean 1.15) at the rural site and 0.73-1.64 (1.10) at the urban site in this study. These values of CPI are close to unity, reflecting elevated fossil fuel combustion (e.g., coal combustion) is a major source for n-alkanes in the YRD region during winter. The CPI values of our study are comparable to those from Chinese urban areas (ave. 1.16) (Wang et al., 2006b) and Tokyo (1.10-2.80, ave.

19

1.50) (Kawamura et al., 1995) where *n*-alkanes were mainly derived from fossil fuel combustion. In contrast, high CPI values were observed for Mt. Tai (ave. 4.60) (Fu et al., 2008) and Chichi-jima atmosphere (4.50) (Kawamura et al., 2003), where a major part of *n*-alkanes originated from terrestrial higher plant waxes.

Moreover, the percent of wax *n*-alkanes (% wax C_n) are also used to assess the contributions of biogenic versus anthropogenic source emissions and higher values point out large contributions from biogenic sources (Simoneit et al., 2004). The average values of % wax C_n were 6.82 % at the rural and 6.49 % at the urban site in the present study, which are lower than fossil fuel emissions from Beijing (11.6 %) (Kang et al., 2018) and Guangzhou (17.3 %) (Wang et al., 2016) in winter, reflecting the great contribution of *n*-alkanes from anthropogenic sources. All of the indices recommend that anthropogenic activities (e.g., fossil fuel combustion, BB, etc.) are the dominant emission sources for the contributions of *n*-alkanes in the YRD regions. Furthermore, diurnal variations of *n*-alkanes are comparable with levoglucosan and PAHs (Fig. 5e-f) which can further prove the emission sources of *n*-alkanes from BB and fossil fuel combustions. In addition, *n*-alkanes showed significant positive correlations with PAHs (r = 0.73, 0.51; P<0.001 for rural and urban, respectively) (Fig. S2a-b) and levoglucosan (r = 0.41 and 0.75; P<0.001 for rural and urban, respectively) (Fig. S2c-d), implying that *n*-alkanes mainly derived from fossil fuel combustion and BB emissions which is consistent with above all the findings.

3.4 Inorganic ions

Inorganic ions are generally water-soluble and contribute to about one-third of the particle mass and play an important role in the environmental changes (Yao et al., 2002; Wang et al., 2005). The values of individual ionic species measured in the rural and urban samples in eastern China are given in Table 2. NO_3^- was found as the dominant ionic species and its concentrations were 28.8 μg m^{-3} and 30.7 μg m^{-3}, accounting for 37.1 % and 34.6 % of

the total measured ionic mass at the rural and urban areas, respectively. The second most

abundant species was found to be SO_4^{2-} (23.6 µg m^{-3} and 25.8 µg m^{-3} at the rural and urban

sites, respectively) followed by NH_4^+ (17.0 µg m^{-3} and 21.1 µg m^{-3}), Cl$^-$, Ca^{2+}, K^+, Na^+, Mg^{2+},

and NO_2^-. All of the major ions showed higher concentrations at the urban site (Fig. 9c),

which is reasonable because of the more anthropogenic/industrial activities. SIA (NO_3^-, SO_4^{2-}

, NH_4^+) contributed almost 90% to the total ionic mass, demonstrating the substantial

formation of secondary aerosols in the YRD region in winter. This result is consistent with

the high concentrations of precursors (NO_x, SO_2, NH_3) in winter from fossil fuel combustion

in the NCP, YRD regions (Yan et al., 2015; Lu et al., 2010) while SO_4^{2-} and NO_3^- primarily

formed through atmospheric oxidation of SO_2 and NO_x, respectively (Seinfeld and Pandis,

2006). The major source of NH_3 are from agricultural activities and vehicular exhaust in

Chinese urban area (Chang et al., 2016), whereas NH_4^+ has other sources also i.e.,

volatilization of animal waste, BB, and emissions from human excreta (Pavuluri et al., 2011a;

Aneja et al., 2012).

The contributions of nss-SO_4^{2-}, nss-K^+ and nss-Ca^{2+} (estimated according to Ni et al.,

2013) to the total SO_4^{2-}, K^+, and Ca^{2+} values were on average more than 99 %, 98 % and

98%, respectively for both sampling sites, indicating minor contributions from marine

compared to anthropogenic sources. The values of ionic species in this study, particularly

NO_3^-, SO_4^{2-} and NH_4^+ are comparable to those reported in the NCP (NO_3^-, 26.1 µg m^{-3}; SO_4^{2-},

28.1 µg m^{-3} and NH_4^+, 21.4 µg m^{-3}) (Li et al., 2017) and Kathmandu Valley, Nepal (NO_3^-,

9.47 µg m^{-3}; SO_4^{2-}, 27.3 µg m^{-3} and NH_4^+, 17.5 µg m^{-3}) (Wan et al., 2019); however, 2-20

times higher than Chennai, India (NO_3^-, 0.88 µg m^{-3}; SO_4^{2-}, 8.70 µg m^{-3} and NH_4^+, 2.06 µg m^{-3}) (Pavuluri et al., 2011a) and Sapporo, Japan (NO_3^-, 1.22 µg m^{-3}; SO_4^{2-}, 3.47 µg m^{-3} and

NH_4^+, 0.68 µg m^{-3}) (Pavuluri et al., 2015). The higher concentrations of SIA implying that

large emissions of their precursors (e.g., NO_x, SO_2 and NH_3, etc.) from anthropogenic

activities (fossil fuel combustion and BB) and favorable meteorological conditions in winter play a major role to form SIA in the atmosphere. It is noteworthy that NO_x, SO_2 and NH_3 are the primary precursors to form new particles such as NO_3^-, SO_4^{2-} and NH_4^+ contributed 40-57 % to $PM_{2.5}$ in China (Yang et al., 2011). Kunwar et al. (2014) proposed that NO_3^-, SO_4^{2-} and NH_4^+ were dominant in winter over the western North Pacific Rim when pollutants originated from fossil fuel combustion, BB and industrial emissions in East Asia.

Nss-K^+ is generally considered as another tracer of BB (Sullivan et al., 2011); however, K^+ has other sources also e.g., soil dust, vegetation and meat cooking, etc. (Zhang et al., 2010). Nss-K^+ showed a significant correlation with levoglucosan at the rural (r = 0.48, p<0.001) and urban sites (r = 0.78, p<0.001), suggesting major part of K^+ originated from BB emissions. Less correlation coefficient (r-value) for rural samples indicates that K^+ partly derived from additional sources such as soil dust and/or vegetation in the rural area. A significant positive correlation was found between rural and urban samples for SIA species (r = 0.59-0.63, p<0.001) (e.g., SO_4^{2-}; Fig. 8e), demonstrating that similar formation pathway concurred to form regional secondary aerosols, possibly due to the influence by meteorological factors (e.g., RH%). A significant Pearson correlation coefficient was also observed for nss-Ca^{2+} (r = 0.70, p<0.001) (Fig. 8f), indicating regional dust transport influence the atmospheric aerosols. This result is invariable with dust episode including similar temporal trends, which was observed during 2015.01.18,10:00 to 2015.01.12,16:00 for both sampling locations (Fig. 11c). Although the urban area's level (mean 2.88 μg m^{-3}) was higher than the rural site (1.41 μg m^{-3}) (Fig. 9c) probably due to the local construction activities.

As the above sections discussed the regional severe haze pollution as well as dust event during the sampling period, a high abundance of ionic species, particularly SIA components (e.g., SO_4^{2-}) were observed during haze pollution (Fig. 6g-h). The concentrations

of SO_4^{2-}, NO_3^- and NH_4^+ were found to be 2-3 times higher in haze days than those of dust days and clear days (Table 3). On the contrary, nss-Ca^{2+} exhibited 4-15 times higher value during dust event (5.36 μg m^{-3} at the rural site and 6.70 μg m^{-3} at the urban site) compared to haze (0.39 μg m^{-3} and 1.50 μg m^{-3}) and clear days (0.38 μg m^{-3} and 1.09 μg m^{-3}) (Table 3 and Fig. 6i-j). Figure 6g-j shows that higher 95th percentile values were observed for SIA species in haze episode, whereas nss-Ca^{2+} was the dominant species during the dust event. It reveals that secondary aerosols play a crucial role in haze formation, resulting in high pollution in the YRD regions. Li et al. (2017) pointed out that primary emissions from coal combustions and BB as well as SO_4^{2-} formation from SO_2 (originated from coal combustions) are the important driving factors to form haze pollution in the NCP region.

3.5 Secondary aerosol formation

Secondary pollutants including secondary organic and inorganic aerosol are formed via homo and heterogeneous chemical reactions in the atmosphere which can substantially affect the air quality. The formation mechanism of secondary aerosol, particularly SOA is very complex and still poorly understood. SOC was estimated using EC-tracer method (Castro et al., 1999; Lim and Turpin, 2002) when the concentrations were found to be 0.54-37.4 μgC m^{-3} (mean 12.9 μgC m^{-3}) at the rural site and 0.16-29.3 μgC m^{-3} (11.7 μgC m^{-3}) at the urban site, accounting for 59 % and 56 % of OC, respectively. The value of SOC was observed around 2-3 times higher during haze days (mean, 16.9 μgC m^{-3} for rural and 15.3 μgC m^{-3} for urban) compared to dust (11.0 and 9.45 μgC m^{-3}) and clear days (6.0 and 6.41 μgC m^{-3}) (Fig. 6e-f), reflecting the substantial formation of SOA during the haze period. A recent study has documented that SOA contributed 30.2 % to organic matter (OM) in winter at a suburban site in the YRD region when local BB emissions influenced the SOA yield (Huang et al., 2013). Furthermore, SOA from BB contributed 10 % to OC and 7 % to fine particle mass in winter at a rural site in northern Italy (Gilardoni et al., 2011).

The SOC results of this study are consistent with liquid water content (LWC) while values were 1 order of magnitude higher during haze period (256 μg m^{-3}) than dust (25.1 μg m^{-3}) and clear days (42.3 μg m^{-3}) at the rural site and 5 times higher during haze period (103 μg m^{-3}) compared to dust (23.0 μg m^{-3}) and clear days (28.7 μg m^{-3}) at the urban site. SOC and LWC exhibited a higher peak during the haze period for both sampling sites as shown in Fig. 7b-c. These results indicate that aqueous phase chemistry plays an important role to form SOA in the YRD region. Because aerosol LWC is a key factor to control the aqueous phase formation of aerosol in the atmosphere (Carlton et al., 2006; Ervens et al., 2008). Moreover, aerosol LWC largely affects the partitioning of water-soluble organic compounds and thus substantially contributes to SOA formation (Hodas et al., 2014). Gilardoni et al. (2016) pointed out that aqueous SOA from residential wood combustion accounted for 4-20 % of the total OA mass in Europe. Previous studies have documented that anthropogenic inorganic species (acidic) e.g., SO_4^{2-}, NO_3^- control aerosol LWC significantly and regulate the transformation of water-soluble gaseous organic precursors to surface of the deliquescent aerosol particle and/or to cloud water (Faust et al., 2017). Recent studies have reported the role of anthropogenic SO_4^{2-} over the southeastern U.S.A and NO_3^- from Po Valley, Italy in controlling the aerosol LWC (Hodas et al., 2014; Carlton et al., 2013).

SIA (i.e., SO_4^{2-}, NO_3^- and NH_4^+) are also an important part of fine particulate matter (PM$_{2.5}$), which have potential impacts on air quality and human health. Detailed results of inorganic species are interpreted in section 3.4. SIA is formed generally through the oxidation and neutralization of sulfur dioxide (SO$_2$), nitrogen oxides (NO$_x$), and ammonia (NH$_3$). Different formation paths of NO_3^- for day and night are observed by the gas-phase oxidation of OH and the hydrolysis of nitrogen pentoxide (N$_2$O$_5$), respectively (Fu et al., 2016a). Huang et al. (2014) reported that severe haze pollution occurred by the formation of secondary aerosol, which contributed 30-77 % and 44-71 % to PM$_{2.5}$ and OA, respectively, in Beijing,

Shanghai, Guangzhou and Xi'an cities during winter when SOA and SIA both were important (SOA/SIA = 0.6-1.4). In the present study, SIA exhibited similar temporal trends with SOC during severe haze pollution days, suggesting influenced by LWC (Figs. 7b-c and 11a-b). Similar diurnal variations were observed for SOC and SIA (e.g., SO_4^{2-}) for both sampling sites while characterized by high peaks at the daytime due to a greater extent of photochemical oxidation (Figs. 4g-h and 5g-h) although higher BLHs were observed at the daytime (see section 3.1). Significant correlations were also found between SOC and SIA (r = 0.65-0.79, p<0.001) and (0.63-0.86, p<0.001) at the rural and urban sites, respectively (Fig. S2e-f). These results demonstrate that the formation of SOA and SIA follow a similar pathway when impacted by meteorological factors (see section 3.1). Diurnal variations of K^+ (primary product) can be further confirmed photochemical oxidation of SIA during the daytime because K^+ was not showing high values at daytime (Fig. 5i-j).

3.6 Stable carbon ($\delta^{13}C$) and nitrogen ($\delta^{15}N$) isotopic composition of aerosols

Stable isotopic compositions of bulk carbon and nitrogen ($\delta^{13}C$ and $\delta^{15}N$) of aerosol particles are used to assess the sources and formation pathways of OAs (Pavuluri et al., 2011b; Aggarwal et al., 2013; Kirillova et al., 2013) although there is overlap in their range values for every defined source. The mean value of $\delta^{13}C$ for TC at the rural samples was found to be −25.3 ‰ with a range of −26.6 ‰ to −22.3 ‰, whereas the same value of −25.3 ‰ (mean) with a range of −27.4 ‰ to −22.3 ‰ was observed for the urban samples. These values are comparable with those reported from the suburban area in Northern Beijing (He et al., 2015), an urban area in Beijing (Ren et al., 2018) and Mumbai city, India (Aggarwal et al., 2013) where fossil fuel combustion and C3 plants burning were considered as the dominant sources. Narukawa et al. (2008) also proposed that arctic aerosols extensively influenced by the continental anthropogenic pollution with the $\delta^{13}C$ value of −25.7±0.7 ‰ when Tokyo urban aerosols showed similar $\delta^{13}C$ value (−25.0±0.8 ‰) of TC. In addition, a

slightly higher $\delta^{13}C$ value of TC (–27.3 ‰) was found in Vancouver tunnel aerosols (relatively fresh from traffic), whereas no significant differences between OC and EC fraction (Huang et al., 2006). This value is comparable with our $\delta^{13}C$ value of urban samples (upper range −27.4 ‰), which is reasonable because of the more traffic emissions in the urban area. Martinelli et al. (2002) reported the $\delta^{13}C$ value of −25.8±0.5 ‰ from the C3 plant dominated region in southeast Brazil. On the contrary, the $\delta^{13}C$ value of TC ranged −23.13 ‰ to −26.40 ‰ was observed from coal combustions and motor vehicles in the Chinese urban area (Cao et al., 2011).

The higher values of $\delta^{13}C$ were observed during dust events (2015.01.18,10:00 to 2015.01.12, 16:00) at the rural (−22.8 ‰ to −25.9 ‰, mean −24.5 ‰) and urban site (−22.3 ‰ to −27.0 ‰, 25.1 ‰) (Fig. 11c-d) might be influenced by regional soil dust contribution. A significant positive correlation was also found between $\delta^{13}C$ and Ca^{2+} for both the rural (r = 0.80, P<0.001) and urban (r = 0.71, P<0.001) samples (Fig. S2g-h) during dust episode, which imply that dust derived carbonate carbon potentially affects the $\delta^{13}C$ ratios in this study. Kawamura and Watanabe (2004) pointed out that $\delta^{13}C$ values of TC increased with an increment of Ca^{2+} concentration (during Asian dust event) in Gosan, South Korea aerosol samples. The profound positive correlation coefficient (r = 0.74, P<0.001) was found for the $\delta^{13}C$ value of TC between rural and urban samples, demonstrating that similar formation process or source emissions affect the carbonaceous aerosols compositions in this study area.

In the present study, daytime $\delta^{13}C$ values were higher than nighttime for both sampling locations while similar diurnal variability was exhibited for SOC (Fig. 4g-j), reflecting that the enrichment of $\delta^{13}C$ during daytime due to the photochemical aging. Recent studies have documented that the values of $\delta^{13}C$ of TC are increased with aerosol photochemical aging (Wang et al., 2010; Aggarwal et al., 2013). Generally, organic compounds discharge CO_2/CO when reaction with OH radicals, resulting in the evolved

species increased with the lighter isotope (^{12}C) and the rest part of organic matter enriched in the heavier isotope (^{13}C) due to kinetic isotope effects (KIEs) (Hoefs, 1997; Aggarwal et al., 2013). Hence, the increment of ^{13}C in an aerosol can broadly be ascribed to aerosol photochemical aging; however, the initial value of δ^{13}C depends on their sources. Similarly, the enrichment of ^{13}C occurred by photochemical oxidation was also reported for dicarboxylic acids (e.g., oxalic acid, one of the dominant photo-oxidized products in the aerosol) from remote marine (Wang and Kawamura, 2006) and East Asia continent (Aggarwal and Kawamura, 2008). The above discussions demonstrate that δ^{13}C values of TC in this study are consistent with the values acquired for aerosol particles from the mixed anthropogenic activities such as BB and fossil fuel combustions, which are invariable with tracer composition results (see section 3.3). It is also important to note that the δ^{13}C values from these sources getting high during daytime due to the photochemically aged when pollution levels were high (Fig. 4), indicating secondary aerosol formation control the regional pollution levels in the YRD region during winter.

The values of δ^{15}N of TN in aerosol particles provide crucial information about the nitrogen sources either primary or secondary (Kundu et al., 2010b; Pavuluri et al., 2010). The δ^{15}N values of TN were found to be −9.6 ‰ to +13.7 ‰ (mean +0.87 ‰) at the rural samples and −6.2 ‰ to +11.6 ‰ (+1.5 ‰) at the urban samples. The δ^{15}N values are lower than a suburban area in Beijing, China (He et al., 2015) and urban area in Chennai, India (Pavuluri et al., 2010) but similar wide range values (−15 ‰ to +12.5 ‰) were observed from the semi-rural area in the UK (Kelly et al., 2005). The higher δ^{15}N values were observed during dust event for both sampling sites (+6.2 ‰ for rural and +5.6 ‰ for urban), whereas low values (e.g., negative values mostly) were exhibited during haze days such as −0.8 ‰ for rural and −0.04 ‰ for the urban site. These results reveal that during dust episode soil nitrogen might contribute to the aerosol particles, in contrast in the heavy haze days, anthropogenic activities

e.g., fossil fuel combustion and BB emit substantial amounts of nitrogen in the atmosphere (see NO_3^- sources in section 3.4). Kundu et al. (2010a) and Kelly et al. (2005) reported isotopic compositions of nitrogen from soil source more than +5.0 ‰ while negative $\delta^{15}N$ values of TN were noted from coal combustion, although C3 plants burning showed values up to +20.0 ‰ (Widory, 2007).

4. Summary and conclusions

PM$_{2.5}$ samples were collected simultaneously from rural and urban areas located in the YRD region in eastern China during winter on 15-28 January 2015. Carbonaceous components, organic tracers (levoglucosan, PAHs, hopanes, and *n*-alkanes), water-soluble inorganic ions, $\delta^{13}C$ of TC and $\delta^{15}N$ of TN were identified in the present study. The concentrations of PM$_{2.5}$ and OC at the rural and urban sites were 2 times higher during haze than clear days, suggesting serious pollution occurred during haze period in the YRD area. Moreover, rural and urban samples exhibited similar temporal trends and a remarkable correlation (r = 0.60, p<0.001) for PM mass, indicating pollution sources or their formation pathways are mostly the same. Diurnal variations of chemical species demonstrated that high pollution raised in the daytime due to the photochemical oxidation process. Moreover, OC and SOC potentially dependent on the relative humidity (RH%) and temperature (T °C) suggesting that meteorological factors largely influenced the air pollution levels.

Levoglucosan is a specific tracer of BB, which was exhibited 2-3 times higher in haze days compared to clear days during the campaign, indicating a large effect of haze pollution by BB emission. LMW-PAHs (3- and 4-rings) were abundant for both sampling sites when PAHs showed a significant correlation with levoglucosan (r = 0.49 and 0.63, p<0.001). It reflects that PAHs mainly emitted from coal combustion and BB emissions of house heating and cooking because more LMW-PAHs are emitted due to low combustion efficiency. The diagnostic ratios of PAHs and hopanes also suggest that they are mainly derived from coal

28

combustion and vehicular exhaust emission, whereas *n*-alkanes emitted from the anthropogenic sources e.g., fossil fuel combustion and BB emission. The molecular distributions of *n*-alkanes were identified by weak odd-carbon-numbered predominance with a maximum at C_{21} and mean CPI values at 1.15 and 1.10, which are close to unity, demonstrating substantial contributions of *n*-alkanes from anthropogenic sources. The % wax *n*-alkanes were observed 6.82 % (rural) and 6.49 % (urban), whereas *n*-alkanes showed significant correlation and similar diurnal patterns with levoglucosan and PAHs, reflecting that *n*-alkanes mainly emitted from fossil fuel combustion and BB emissions.

SOC and SIA along with LWC exhibited a higher peak during haze period for both sampling sites while SOC showed a profound correlation with SIA, indicating aqueous phase chemistry plays an important role to enhance secondary aerosols during haze days. However, similar diurnal variations with the higher concentrations at daytime were observed for SOC and SIA, implying photochemical oxidation also significantly affect secondary aerosol formation. SOC and SIA contributed almost 60 % and 90 % to the OC and total ionic mass, respectively, suggesting the substantial formation of secondary aerosols in the sampling area. Furthermore, meaningful correlation coefficients were observed between rural and urban samples for SIA species i.e., SO_4^{2-} (r = 0.63, p<0.001), NO_3^- (r = 0.59, p<0.001) and NH_4^+ (r = 0.64, p<0.001), indicating that similar formation pathway occurred to form regional secondary aerosols, probably due to the influence by meteorological factors (e.g., RH%). A significant correlation coefficient was also found between both sampling sites for nss-Ca^{2+}, indicating regional dust transport affects the atmospheric pollution levels. The values of stable carbon isotope compositions of TC ($\delta^{13}C$) in this study revealed that anthropogenic activities such as fossil fuel combustion and BB are the dominant sources for carbonaceous aerosols. In contrast, values of stable nitrogen isotope compositions of TN ($\delta^{15}N$)

demonstrated that soil nitrogen along with fossil fuel combustion and BB are the major

sources for nitrogenous aerosols.

Most of the organic compounds were dominant in the rural site, whereas PM mass,

OC, EC, and inorganic species were more abundant in the urban samples, indicating the

urban atmosphere is more affected by industrial/anthropogenic emissions. The results of this

study demonstrate that regional anthropogenic sources and meteorological factors (e.g., RH,

temperature, etc.) enhance the pollution levels during haze event in the YRD region in eastern

China, which affect the regional climate.

References

Adame, J. A., Notario, A., Villanueva, F. and Albaladejo, J.: Application of cluster analysis
to surface ozone, NO2 and SO2 daily patterns in an industrial area in Central-Southern
Spain measured with a DOAS system, Sci. Total Environ., doi:10.1016/j.scitotenv.
2012.04.032, 2012.

Adler, G., Flores, J. M., Abo Riziq, A., Borrmann, S. and Rudich, Y.: Chemical, physical,
and optical evolution of biomass burning aerosols: A case study, Atmos. Chem. Phys.,
11(4), 1491–1503, doi:10.5194/acp-11-1491-2011, 2011.

Aggarwal, S. G. and Kawamura, K.: Molecular distributions and stable carbon isotopic
compositions of dicarboxylic acids and related compounds in aerosols from Sapporo,
Japan: Implications for photochemical aging during long-range atmospheric transport, J.
Geophys. Res., 113(D14), D14301Doi 10.1029/2007jd009365, 2008.

Aggarwal, S. G., Kawamura, K., Umarji, G. S., Tachibana, E., Patil, R. S. and Gupta, P. K.:
Organic and inorganic markers and stable C-, N-isotopic compositions of tropical coastal
aerosols from megacity Mumbai: Sources of organic aerosols and atmospheric
processing, Atmos. Chem. Phys., doi:10.5194/acp-13-4667-2013, 2013.

Andreae, M. O. and Merlet, P.: Emission of trace gases and aerosols from biomass burning,
Glob. Biogeochem. Cycles, 15, 955–966, 2001.

Aneja, V. P., Schlesinger, W. H., Erisman, J. W., Behera, S. N., Sharma, M. and Battye, W.: Reactive nitrogen emissions from crop and livestock farming in India, Atmos. Environ., doi:10.1016/j.atmosenv.2011.11.026, 2012.

Bao, M., Cao, F., Chang, Y., Zhang, Y. L., Gao, Y., Liu, X., Zhang, Y., Zhang, W., Tang, T., Xu, Z., Liu, S., Lee, X., Li, J. and Zhang, G.: Characteristics and origins of air pollutants and carbonaceous aerosols during wintertime haze episodes at a rural site in the Yangtze River Delta, China, Atmos. Pollut. Res., doi:10.1016/j.apr.2017.03.001, 2017.

Bergin, M. H., Cass, G. R., Xu, J., Fang, C., Zeng, L. M., Yu, T., Salmon, L. G., Kiang, C. S., Tang, X. Y., Zhang, Y. H. C. and L., W.: Aerosol radiative, physical, and chemical properties in Beijing during June 1999., J. Geophys. Res., 106 (D16), 17969–17980, 2001.

Bi, X., Sheng, G., Peng, P., Chen, Y. and Fu, J.: Size distribution of n-alkanes and polycyclic aromatic hydrocarbons (PAHs) in urban and rural atmospheres of Guangzhou, China, Atmos. Environ., 39(3), 477–487, doi:10.1016/j.atmosenv.2004.09.052, 2005.

Bond, T.C., Streets, D.G., Yarber, K.F., Nelson, S.M., Woo, J.-H., and Klimont, Z.: A technology-based global inventory of black and organic carbon emissions from combustion, J. Geophys. Res., 109(D14203), doi:10.1029/2003JD003697, 2004.

Boreddy, S. K. R., Haque, M., Kawamura, K., Fu, P. and Kim, Y.: Homologous series of n-alkanes (C19-C35), fatty acids (C12-C32) and n-alcohols (C8-C30) in atmospheric aerosols from central Alaska: Molecular distributions, seasonality and source indices, Atmos. Environ., 184(November 2017), 87–97, doi:10.1016/j.atmosenv.2018.04.021, 2018.

Bourotte, C., Forti, M. C., Taniguchi, S., Bícego, M. C. and Lotufo, P. A.: A wintertime study of PAHs in fine and coarse aerosols in São Paulo city, Brazil, Atmos. Environ., doi:10.1016/j.atmosenv.2005.02.054, 2005.

Cao, F., Zhang, S. C., Kawamura, K. and Zhang, Y. L.: Inorganic markers, carbonaceous components and stable carbon isotope from biomass burning aerosols in Northeast China, Sci. Total Environ., doi:10.1016/j.scitotenv.2015.09.099, 2016.

Cao, J., Chow, J. C., Tao, J., Lee, S., Watson, J. G., Ho, K., Wang, G., Zhu, C. and Han, Y.: Stable carbon isotopes in aerosols from Chinese cities: Influence of fossil fuels, Atmos. Environ., doi:10.1016/j.atmosenv.2010.10.056, 2011.

Carlton, A. G., Turpin, B. J., Lim, H. J., Altieri, K. E. and Seitzinger, S.: Link between isoprene and secondary organic aerosol (SOA): Pyruvic acid oxidation yields low volatility organic acids in clouds, Geophys. Res. Lett., 33, L06822(6), L06822, Doi 10.1029/2005gl025374, 2006.

Carlton, A. G. and Turpin, B. J.: Particle partitioning potential of organic compounds is highest in the Eastern US and driven by anthropogenic water, Atmos. Chem. Phys., doi:10.5194/acp-13-10203-2013, 2013.

Cass, G. R.: Organic molecular tracers for particulate air pollution sources, TrAC - Trends Anal. Chem., doi:10.1016/S0165-9936(98)00040-5, 1998.

Castro, L. M., Pio, C. A., Harrison, R. M. and Smith, D. J. T.: Carbonaceous aerosol in urban and rural European atmospheres: estimation of secondary organic carbon concentrations, Atmos. Environ., 33(17), 2771–2781, 1999.

Chang, Y., Zou, Z., Deng, C., Huang, K., Collett, J. L., Lin, J. and Zhuang, G.: The importance of vehicle emissions as a source of atmospheric ammonia in the megacity of Shanghai, Atmos. Chem. Phys., doi:10.5194/acp-16-3577-2016, 2016.

Chang, Y., Deng, C., Cao, F., Cao, C., Zou, Z., Liu, S., Lee, X., Li, J., Zhang, G. and Zhang, Y.: Assessment of carbonaceous aerosols in Shanghai, China-Part 1: Long-term evolution, seasonal variations, and meteorological effects, Atmos. Chem. Phys., doi:10.5194/acp-17-9945-2017, 2017.

Chen, Y., Tian, C., Feng, Y., Zhi, G., Li, J. and Zhang, G.: Measurements of emission factors of PM2.5, OC, EC, and BC for household stoves of coal combustion in China, Atmos. Environ., doi:10.1016/j.atmosenv.2015.03.023, 2015.

Cheng, Y., Engling, G., He, K.-B., Duan, F.-K., Ma, Y.-L., Du, Z.-Y., Liu, J.-M., Zheng, M., and Weber, R. J.: Biomass burning contribution to Beijing aerosol, Atmos. Chem. Phys., 13, 7765–7781, 2013.

Cooke, W. F., Liousse, C., Cachier, H. and Feichter, J.: Construction of a 1 degrees x 1 degrees fossil fuel emission data set for carbonaceous aerosol and implementation and radiative impact in the ECHAM4 model, J. Geophys. Res., [Atmos], 104(D18), 22137–22162, 1999.

Ding, L. C., Fu K., Daniel, K. W., Wang, Tom Dann, C. C. A.: A new direct thermal desorption-GC/MS method: Organic speciation of ambient particulate matter collected in Golden, BC, Atmos. Environ., 43, 4894–4902, 2009.

Ding, X., He, Q. F., Shen, R. Q., Yu, Q. Q. and Wang, X. M.: Spatial distributions of secondary organic aerosols from isoprene, monoterpenes, β-caryophyllene, and aromatics over China during summer, J. Geophys. Res., doi:10.1002/2014JD021748, 2014.

Du, H., Kong, L., Cheng, T., Chen, J., Du, J., Li, L., Xia, X., Leng, C. and Huang, G.: Insights into summertime haze pollution events over Shanghai based on online water-soluble ionic composition of aerosols, Atmos. Environ., doi:10.1016/j.atmosenv.2011.06.027, 2011.

Ervens, B., Carlton, A. G., Turpin, B. J., Altieri, K. E., Kreidenweis, S. M. and Feingold, G.: Secondary organic aerosol yields from cloud-processing of isoprene oxidation products, Geophys. Res. Lett., 35, GL0318(2), doi:10.1029/2007GL031828, 2008.

Falkovich A. H., Graber, E. R., Schkolnik, G., Rudich, Y., Maenhaut, W. and Artaxo, P.: Low molecular weight organic acids in aerosol particles from Rondˆonia, Brazil, during the biomass-burning, transition and wet periods, Atmos. Chem. Phys., (5), 781–797, 2005.

Fan, M. Y., Zhang, Y. L., Lin, Y. C., Chang, Y. H., Cao, F., Zhang, W. Q., Hu, Y. B., Bao, M. Y., Liu, X. Y., Zhai, X. Y., Lin, X., Zhao, Z. Y. and Song, W. H.: Isotope-based source apportionment of nitrogen-containing aerosols: A case study in an industrial city in China, Atmos. Environ., doi:10.1016/j.atmosenv.2019.05.020, 2019.

Faust, J. A., Wong, J. P. S., Lee, A. K. Y. and Abbatt, J. P. D.: Role of Aerosol Liquid Water in Secondary Organic Aerosol Formation from Volatile Organic Compounds, Environ. Sci. Technol., doi:10.1021/acs.est.6b04700, 2017.

Feng, J. L., Chan, C. K., Fang, M., Hu, M., He, L. Y. and Tang, X. Y.: Characteristics of organic matter in PM2.5 in Shanghai, Chemosphere, 64(8), 1393–1400, 2006.

Fraser, M. P. and Lakshmanan, K.: Using levoglucosan as a molecular marker for the long-range transport of biomass combustion aerosols, Environ. Sci. Technol., 34, 4560–4564, 2000.

Forster, P., Ramaswamy, V., Artaxo, P., Berntsen, T., Betts, R., Fahey, D. W., Haywood, J., Lean, J., Lowe, D. C., Myhre, G., Nganga, J., Prinn, R., Raga, G., Schulz, M., and Van Dorland, R.: Changes in Atmospheric Constituents and in Radiative Forcing, in: Climate Change 2007: The Physical Science Basis, contribution of Working Group I to the Fourth Assessment Report of the Intergovernmental Panel on Climate Change, edited by: Solomon, S. D., Qin, M., Manning, Z., Chen, M., Marquis, K. B., Averyt, M. T., and Miller, H. L., Cambridge University Press, Cambridge, United Kingdom and New York, NY, USA, 129-134, 2007.

Fu, P. Q., Kawamura, K., Okuzawa, K., Aggarwal, S. G., Wang, G., Kanaya, Y. and Wang, Z.: Organic molecular compositions and temporal variations of summertime mountain

aerosols over Mt. Tai, North China Plain, J. Geophys. Res., [Atmos], 113, D1910, doi:10.1029/2008JD009900, 2008.

Fu, P. Q., Kawamura, K., Cheng, Y. F., Hatakeyama, S., Takami, A., Li, H. and Wang, W.: Aircraft measurements of polar organic tracer compounds in tropospheric particles (PM10) over central China, Atmos. Chem. Phys., doi:10.5194/acp-14-4185-2014, 2014.

Fu, X., Wang, S., Chang, X., Cai, S., Xing, J. and Hao, J.: Modeling analysis of secondary inorganic aerosols over China: Pollution characteristics, and meteorological and dust impacts, Sci. Rep., doi:10.1038/srep35992, 2016a.

Fu, X., Zhen C., Shuxiao W., Yang H., and Xing, J. H.: Local and Regional Contributions to Fine Particle Pollution in Winter of the Yangtze River Delta, China, Aerosol Air Qual. Res., 16, 1067–1080, doi:10.4209/aaqr.2015.08.0496, 2016b.

Gilardoni, S., Vignati, E., Cavalli, F., Putaud, J. P., Larsen, B. R., Karl, M., Stenstr Ãm, K., Genberg, J., Henne, S. and Dentener, F.: Better constraints on sources of carbonaceous aerosols using a combined ^{14}C-macro tracer analysis in a European rural background site, Atmos. Chem. Phys., doi:10.5194/acp-11-5685-2011, 2011.

Gilardoni, S., Massoli, P., Paglione, M., Giulianelli, L., Carbone, C., Rinaldi, M., Decesari, S., Sandrini, S., Costabile, F., Gobbi, G. P., Pietrogrande, M. C., Visentin, M., Scotto, F., Fuzzi, S. and Facchini, M. C.: Direct observation of aqueous secondary organic aerosol from biomass-burning emissions, Proc. Natl. Acad. Sci., doi:10.1073/pnas.1602212113, 2016.

Grimmer, G., Jacob, J., and Noujack, K. W.: Profile of the polycyclic aromatic hydrocarbons from lubricating oils. Inventory by GC/MS-PAH in environmental materials, part 1., Fresenius Zeitschrift fur Anal. Chemie, 314, 13–19., 1983.

Guenther, A., Karl, T., Harley, P., Wiedinmyer, C., Palmer, P. I. and Geron, C.: Estimates of global terrestrial isoprene emissions using MEGAN (Model of Emissions of Gases and Aerosols from Nature), Atmos. Chem. Phys., 6, 3181–3210, 2006.

He, L. Y., Hu, M., Zhang, Y. H., Huang, X. F. and Yao, T. T.: Fine particle emissions from on-road vehicles in the Zhujiang Tunnel, China, Environ. Sci. Technol., doi:10.1021/es7022658, 2008.

He, N., Kawamura, K., Kanaya, Y. and Wang, Z.: Diurnal variations of carbonaceous components, major ions, and stable carbon and nitrogen isotope ratios in suburban aerosols from northern vicinity of Beijing, Atmos. Environ., doi:10.1016/j.atmosenv. 2015.10.052, 2015.

Hemming, B. L. and Seinfeld, J. H.: On the hygroscopic bahavior of atmospheric organic aerosols, Ind. Eng. Chem. Res., 40(20), 4162–4171, 2001.

Hodas, N., Sullivan, A. P., Skog, K., Keutsch, F. N., Collett, J. L., Decesari, S., Facchini, M. C., Carlton, A. G., Laaksonen, A. and Turpin, B. J.: Aerosol liquid water driven by anthropogenic nitrate: Implications for lifetimes of water-soluble organic gases and potential for secondary organic aerosol formation, Environ. Sci. Technol., doi:10.1021/es5025096, 2014.

Hoefs, J.: Stable Isotope Geochemistry, Springer, New York., 1997.

Hu, T., Zhang, J., Xing, X., Zhan, C., Zhang, L., Liu, H., Liu, T., Zheng, J., Yao, R. and Cao, J.: Seasonal variation and health risk assessment of atmospheric PM 2.5 -bound polycyclic aromatic hydrocarbons in a classic agglomeration industrial city, central China, Air Qual. Atmos. Heal., doi:10.1007/s11869-018-0575-3, 2018.

Huang, L., Brook, J. R., Zhang, W., Li, S. M., Graham, L., Ernst, D., Chivulescu, A. and Lu, G.: Stable isotope measurements of carbon fractions (OC/EC) in airborne particulate: A new dimension for source characterization and apportionment, Atmos. Environ., 40(15), 2690–2705, 2006.

Huang, X. F., Xue, L., Tian, X. D., Shao, W. W., Sun, T. Le, Gong, Z. H., Ju, W. W., Jiang, B., Hu, M. and He, L. Y.: Highly time-resolved carbonaceous aerosol characterization in Yangtze River Delta of China: Composition, mixing state and secondary formation, Atmos. Environ., doi:10.1016/j.atmosenv.2012.09.059, 2013.

Huang, R. J., Zhang, Y., Bozzetti, C., Ho, K. F., Cao, J. J., Han, Y., Daellenbach, K. R., Slowik, J. G., Platt, S. M., Canonaco, F., Zotter, P., Wolf, R., Pieber, S. M., Bruns, E. A., Crippa, M., Ciarelli, G., Piazzalunga, A., Schwikowski, M., Abbaszade, G., Schnelle-Kreis, J., Zimmermann, R., An, Z., Szidat, S., Baltensperger, U., El Haddad, I. and Prevot, A. S.: High secondary aerosol contribution to particulate pollution during haze events in China, Nature, 514(7521), doi:10.1038/nature13774, 2014.

IPCC (2001). Climate Change 2001: The Scientific Basis- Contribution of Working Group I to the Third Assessment Report of the Intergovernmental Panel on Climate Change. Houghton J.T. et al., (Eds.), Cambridge Univ. Press, New York. 881 pp.

Jones, T., Wlodarczyk, A., Koshy, L., Brown, P., Longyi, S. and Bérubé, K.: The geochemistry and bioreactivity of fly-ash from coal-burning power stations, Biomarkers, doi:10.1080/13547500902965195, 2009.

Kan, H., London, S. J., Chen, G., Zhang, Y., Song, G., Zhao, N., Jiang, L. and Chen, B.: Differentiating the effects of fine and coarse particles on daily mortality in Shanghai, China, Environ. Int., doi:10.1016/j.envint.2006.12.001, 2007.

Kanakidou, M., Seinfeld, J. H., Pandis, S. N., Barnes, I., Dentener, F. J., Facchini, M. C., Van Dingenen, R., Ervens, B., Nenes, A., Nielsen, C. J., Swietlicki, E., Putaud, J. P., Balkanski, Y., Fuzzi, S., Horth, J., Moortgat, G. K., Winterhalter, R., Myhre, C. E. L., Tsigaridis, K., Vignati, E., Stephanou, E. G. and Wilson, J.: Organic aerosol and global climate modelling: a review, Atmos. Chem. Phys., 5, 1053–1123, 2005.

Kang, M., Ren, L., Ren, H., Zhao, Y., Kawamura, K., Zhang, H., Wei, L., Sun, Y., Wang, Z. and Fu, P.: Primary biogenic and anthropogenic sources of organic aerosols in Beijing, China: Insights from saccharides and n-alkanes, Environ. Pollut., doi:10.1016/j.envpol.2018.09.118, 2018.

Kavouras, I. G., Lawrence, J., Koutrakis, P., Stephanou, E. G. and Oyola, P.: Measurement of particulate aliphatic and polynuclear aromatic hydrocarbons in Santiago de Chile: source reconciliation and evaluation of sampling artifacts, Atmos. Environ., 33(30), 4977–4986, 1999.

Kawamura, K., Kosaka, M. and Sempéré, R.: Distributions and seasonal changes of hydrocarbons in urban aerosols and rainwaters, Chikyukagaku (Geochemistry), 29, 1–15, 1995.

Kawamura, K., Ishimura, Y. and Yamazaki, K.: Four years' observations of terrestrial lipid class compounds in marine aerosols from the western North Pacific, Glob. Biogeochem. Cycles, 17, 1003(1), doi:10.1029/2001GB001810, 2003.

Kawamura, K. and Watanabe, T.: Determination of stable carbon isotopic compositions of low molecular weight dicarboxylic acids and keto-carboxylic acids in atmospheric aerosol and snow samples, Anal. Chem., 76(19), 5762–5768, 2004.

Kelly, S. D., Stein, C. and Jickells, T. D.: Carbon and nitrogen isotopic analysis of atmospheric organic matter, Atmos. Environ., 39(32), 6007–6011, 2005.

Khan, M. F., Latif, M. T., Lim, C. H., Amil, N., Jaafar, S. A., Dominick, D., Mohd Nazir, M. S., Sahani, M. and Tahir, N. M.: Seasonal effect and source apportionment of polycyclic aromatic hydrocarbons in PM2.5, Atmos. Environ., doi:10.1016/j.atmosenv.2015.01.077, 2015.

Kim, H., Kim, J. Y., Kim, J. S. and Jin, H. C.: Physicochemical and optical properties of combustion-generated particles from a coal-fired power plant, automobiles, ship engines, and charcoal kilns, Fuel, doi:10.1016/j.fuel.2015.08.035, 2015.

Kirillova, E. N., Andersson, A., Sheesley, R. J., Kruså, M., Praveen, P. S., Budhavant, K., Safai, P. D., Rao, P. S. P. and Gustafsson, Ö.: ^{13}C- And ^{14}C-based study of sources and atmospheric processing of water-soluble organic carbon (WSOC) in South Asian aerosols, J. Geophys. Res. Atmos., doi:10.1002/jgrd.50130, 2013.

Kundu, S., Kawamura, K., Andreae, T. W., Hoffer, A. and Andreae, M. O.: Diurnal variation in the water-soluble inorganic ions, organic carbon and isotopic compositions of total carbon and nitrogen in biomass burning aerosols from the LBA-SMOCC campaign in Rondonia, Brazil, J. Aerosol Sci., 41(1), 118–133, doi:10.1016/j.jaerosci.2009.08.006, 2010a.

Kundu, S., Kawamura, K. and Lee, M.: Seasonal variation of the concentrations of nitrogenous species and their nitrogen isotopic ratios in aerosols at Gosan, Jeju Island: Implications for atmospheric processing and source changes of aerosols, J. Geophys. Res., 115, D20305, Doi 10.1029/2009jd013323, 2010b.

Kunwar, B. and Kawamura, K.: One-year observations of carbonaceous and nitrogenous components and major ions in the aerosols from subtropical Okinawa Island, an outflow region of Asian dusts, Atmos. Chem. Phys., 14, 1819–1836, doi:https://doi.org/10.5194/acp-14-1819-2014, 2014.

Lee, S., Kim, H. K., Yan, B., Cobb, C. E., Hennigan, C., Nichols, S., Chamber, M., Edgerton, E. S., Jansen, J. J., Hu, Y., Zheng, M., Weber, R. J. and Russell, A. G.: Diagnosis of aged prescribed burning plumes impacting an urban area, Environ. Sci. Technol., 42(5), 1438–1444, doi:10.1021/es7023059, 2008.

Li, H., Zhang, Q., Zhang, Q., Chen, C., Wang, L., Wei, Z. and Zhou, S.: Wintertime aerosol chemistry and haze evolution in an extremely polluted city of the North China Plain: significant contribution from coal and biomass combustion, Atmos. Chem. Phys., 4751–4768, doi:10.5194/acp-17-4751-2017, 2017.

Li, L., Ren, L., Ren, H., Yue, S., Xie, Q., Zhao, W., Kang, M., Li, J., Wang, Z., Sun, Y. and Fu, P.: Molecular Characterization and Seasonal Variation in Primary and Secondary Organic Aerosols in Beijing, China, J. Geophys. Res. Atmos., doi:10.1029/2018JD028527, 2018.

Lim, H. J. and Turpin, B. J.: Origins of primary and secondary organic aerosol in Atlanta: Results of time-resolved measurements during the Atlanta Supersite Experiment, Environ. Sci. Technol., doi:10.1021/es0206487, 2002.

Lu, C., Niu, S., Tang, L., Lv, J., Zhao, L. and Zhu, B.: Chemical composition of fog water in Nanjing area of China and its related fog microphysics, Atmos. Res., doi:10.1016/j.atmosres.2010.03.007, 2010.

Martinelli, L. A., Camargo, P. B., Lara, L. B. L. S., Victoria, R. L. and Artaxo, P.: Stable carbon and nitrogen isotopic composition of bulk aerosol particles in a C4 plant landscape of southeast Brazil, Atmos. Environ., doi:10.1016/S1352-2310(01)00454-X, 2002.

Mochida, M., Kawamura, K., Fu, P. and Takemura, T.: Seasonal variation of levoglucosan in aerosols over the western North Pacific and its assessment as a biomass-burning tracer, Atmos. Environ., 44, 3511–3518, 2010.

Narukawa, M., Kawamura, K., Li, S. M. and Bottenheim, J. W.: Stable carbon isotopic rations and ionic composition of the high Arctic aerosols: An increase in δ^{13}C values from winter to spring, J. Geophys. Res., [Atmos], 113(D02312), doi:10.1029/2007JD008755, 2008.

Ni, T., Li, P., Han, B., Bai, Z., Ding, X., Wang, Q., Huo, J. and Lu, B.: Spatial and temporal variation of chemical composition and mass closure of ambient pm 10 in Tianjin, China, Aerosol Air Qual. Res., doi:10.4209/aaqr.2012.10.0283, 2013.

35

Ohura, T., Amagai, T., Fusaya, M. and Matsushita, H.: Polycyclic Aromatic Hydrocarbons in Indoor and Outdoor Environments and Factors Affecting Their Concentrations, Environ. Sci. Technol., 38(1), 77–83, doi:10.1021/es030512o, 2004.

Orasche, J., Schnelle-Kreis, J., Abbaszade, G., and Zimmermann, R., 2011. Technical note: in-situ derivatization thermal desorption GC-TOFMS for direct analysis of particle-bound non-polar and polar organic species. Atmos. Chem. Phys., 11, 8977–8993. https://doi.org/10.5194/acp-11-8977-2011.

Oros, D. R. and Simoneit, B. R. T.: Identification and emission rates of molecular tracers in coal smoke particulate matter, Fuel, 79, 515–536, 2000.

Pavuluri, C. M., Kawamura, K., Tachibana, E. and Swaminathan, T.: Elevated nitrogen isotope ratios of tropical Indian aerosols from Chennai: Implication for the origins of aerosol nitrogen in South and Southeast Asia, Atmos. Environ., 44(29), 3597–3604, doi:Doi 10.1016/J.Atmosenv.2010.05.039, 2010.

Pavuluri, C. M., Kawamura, K., Aggarwal, S. G. and Swaminathan, T.: Characteristics, seasonality and sources of carbonaceous and ionic components in the tropical aerosols from Indian region, Atmos. Chem. Phys., doi:10.5194/acp-11-8215-2011, 2011a.

Pavuluri, C. M., Kawamura, K., Swaminathan, T. and Tachibana, E.: Stable carbon isotopic compositions of total carbon, dicarboxylic acids and glyoxylic acid in the tropical Indian aerosols: Implications for sources and photochemical processing of organic aerosols, J. Geophys. Res., 116, D18307Doi 10.1029/2011jd015617, 2011b.

Pavuluri, C. M., Kawamura, K., Mihalopoulos, N. and Fu, P.: Characteristics, seasonality and sources of inorganic ions and trace metals in North-east Asian aerosols, Environ. Chem., doi:10.1071/en14186, 2015.

Pöschl, U.: Atmospheric aerosols: Composition, transformation, climate and health effects, Angew. Chem. Int. Ed., 44, 7520–7540, 2005.

Reid, J. S., Eck, T. F., Christopher, S. A., Koppmann, R., D. and O., Eleuterio, D. P., Holben, B. N., Reid, E. A., and Zhang, J.: A review of biomass burning emissions part III: intensive optical properties of biomass burning particles, Atmos. Chem. Phys., 5, 827–849, doi:10.5194/acp-5-827-2005, 2005a.

Reid, J. S., Koppmann, R., Eck, T. F., and Eleuterio, D. P.: A review of biomass burning emissions part II: intensive physical properties of biomass burning particles, Atmos. Chem. Phys., 5, 799– 825, doi:10.5194/acp-5-799-2005, 2005b.

Reiss, R., Anderson, E. L., Cross, C. E., Hidy, G., Hoel, D., McClellan, R. and Moolgavkar, S.: Evidence of health impacts of sulfate- and nitrate-containing particles in ambient air, Inhal. Toxicol., doi:10.1080/08958370601174941, 2007.

Ren, H., Kang, M., Ren, L., Zhao, Y., Pan, X., Yue, S., Li, L., Zhao, W., Wei, L., Xie, Q., Li, J., Wang, Z., Sun, Y., Kawamura, K. and Fu, P.: The organic molecular composition, diurnal variation, and stable carbon isotope ratios of PM2.5 in Beijing during the 2014 APEC summit, Environ. Pollut., doi:10.1016/j.envpol.2018.08.094, 2018.

Rogge, W. F., Hildemann, L. M., Mazurek, M. A., Cass, G. R. and Simoneit, B. R. T.: Sources of Fine Organic Aerosol. 2. Noncatalyst and Catalyst-Equipped Automobiles and Heavy-Duty Diesel Trucks, Environ. Sci. Technol., 27(4), 636–651, doi:10.1021/es00041a007, 1993.

Schauer, J. J., Rogge, W. F., Hildemann, L. M., Mazurek, M. A. and Cass, G. R.: Source apportionment of airborne particulate matter using organic compounds as tracers, Atmos. Environ., 30(22), 3837–3855, 1996.

Schauer, J. J., Kleeman, M. J., Cass, G. R. and Simoneit, B. R. T.: Measurement of emissions from air pollution sources. C13-C29 organic compounds from fireplace combustion of wood, Environ. Sci. Technol., 35(9), 1716–1728, 2001.

Schnelle-Kreis, J., Sklorz, M., Orasche, J., Stölzel, M., Peters, A. and Zimmermann, R.: Semi volatile organic compounds in ambient PM2.5. Seasonal trends and daily resolved source contributions, Environ. Sci. Technol., doi:10.1021/es060666e, 2007.

Seinfeld, J. H. & Pandis, S. N.: Atmospheric Chemistry and Physics: From Air Pollution to Climate Change, 2nd edn., Wiley., 2006.

Shao, L., Shi, Z., Jones, T. P., Li, J., Whittaker, A. G. and BéruBé, K. A.: Bioreactivity of particulate matter in Beijing air: Results from plasmid DNA assay, Sci. Total Environ., doi:10.1016/j.scitotenv.2005.10.009, 2006.

Sheesley, R. J., Mark, M., Jeff, T., De, M., Brandon, R. and Shelton, J. J. S.: Development of an in situ derivatization technique for rapid analysis of levoglucosan and polar compounds in atmospheric organic aerosol, Atmos. Environ., 123, 251–255, 2015.

Shrivastava, M., Lou, S., Zelenyuk, A., Easter, R. C., Corley, R. A., Thrall, B. D., Rasch, P. J., Fast, J. D., Massey Simonich, S. L., Shen, H. and Tao, S.: Global long-range transport and lung cancer risk from polycyclic aromatic hydrocarbons shielded by coatings of organic aerosol, Proc. Natl. Acad. Sci., doi:10.1073/pnas.1618475114, 2017.

Simoneit, B. R. T., Cardoso, J. N. and Robinson, N.: An assessment of terrestrial higher molecular weight lipid compounds in aerosol particulate matter over the south Atlantic from about 30-70°S., Chemosphere, 23, 447-465., 1991.

Simoneit, B. R. T.: Biomass burning-a review of organic tracers for smoke from incomplete combustion, Appl. Geochem., 17, 129–162, 2002.

Simoneit, B. R. T., Kobayashi, M., Mochida, M., Kawamura, K., Lee, M., Lim, H. J., Turpin, B. J. and Komazaki, Y.: Composition and major sources of organic compounds of aerosol particulate matter sampled during the ACE-Asia campaign, J. Geophys. Res., [Atmos], 109, D19S1, doi:10.1029/2004JD004598, 2004.

Sklorz, M., Schnelle-Kreis, J., Liu, Y., Orasche, J. and Zimmermann, R: Daytime resolved analysis of polycyclic aromatic hydrocarbons in urban aerosol samples–Impact of sources and meteorological conditions, Chemosphere, 67, 934–943, 2007.

Sullivan Frank, N., Onstad, G., Simpson, C. D., and Collett, A. P.: Application of high-performance anion-exchange chromatography-pulsed amperometric detection for measuring carbohydrates in routine daily filter samples collected by a national network: 1. Determination of the impact of biomass burning in the upper Midwest, J. Geophys. Res., 116, doi:10.1029/2010jd014166, 2011.

Sun, K., Liu, H. N., Ding, A. J. and Wang, X. Y.: WRF-chem simulation of a severe haze episode in the Yangtze River Delta, China, Aerosol Air Qual. Res., 16 (5), 1268–1283, 2016.

Sun, Y. L., Zhang, Q., Anastasio, C. and Sun, J.: Insights into secondary organic aerosol formed via aqueous-phase reactions of phenolic compounds based on high-resolution mass spectrometry, Atmos. Chem. Phys., 10(10), 4809–4822, doi:10.5194/acp-10-4809-2010, 2010.

Sverdrup, L. E, Nielsen, T. and K. P.: Soil ecotoxicity of polycyclic aromatic hydrocarbons in relation to soil sorption, lipophilicity, and water solubility, Environ. Sci. Tec., 36, 2429–2435, 2002.

Syed, J. H., Iqbal, M., Zhong, G., Katsoyiannis, A., Yadav, I. C., Li, J. and Zhang, G.: Polycyclic aromatic hydrocarbons (PAHs) in Chinese forest soils: Profile composition, spatial variations and source apportionment, Sci. Rep., doi:10.1038/s41598-017-02999-0, 2017.

Sha, T., Xiaoyan, M., Hailing, J., Ronald, J. A., Jieying, D., Yanlin, Z. and Chang, Y.: Exploring the influence of two inventories on simulated air pollutants during winter over the Yangtze River Delta, Atmos. Environ., 206, 170–182, 2019.

VanCuren, R. A. and Cahill, T. A.: Asian aerosols in North America: Frequency and concentration of fine dust., J. Geophys. Res., [Atmos], 107 (D24), 484, doi:http://dx.doi.org/10.1029/2002JD002204, 2002.

Wan, X., Kang, S., Rupakheti, M., Zhang, Q., Tripathee, L., Guo, J., Chen, P., Rupakheti, D., Panday, A. K., Lawrence, M. G., Kawamura, K. and Cong, Z.: Molecular characterization of organic aerosols in the Kathmandu Valley, Nepal: Insights into primary and secondary sources, Atmos. Chem. Phys., doi:10.5194/acp-19-2725-2019, 2019.

Wang, G. and Kawamura, K.: Molecular characteristics of urban organic aerosols from Nanjing: A case study of a mega-city in China, Environ. Sci. Technol., 39(19), 7430–7438, 2005.

Wang, G., Kawamura, K., Watanabe, T., Lee, S. C., Ho, K. F. and Cao, J. J.: High loadings and source strengths of organic aerosols in China, Geophys. Res. Lett., 33, L22801, doi:10.1029/2006GL027624, 2006a.

Wang, G., Kawamura, K., Lee, S., Ho, K. F. and Cao, J. J.: Molecular, seasonal, and spatial distributions of organic aerosols from fourteen Chinese cities, Environ. Sci. Technol., 40(15), 4619–4625, 2006b.

Wang, G., Kawamura, K., Zhao, X., Li, Q., Dai, Z. and Niu, H.: Identification, abundance and seasonal variation of anthropogenic organic aerosols from a mega-city in China, Atmos. Environ., 41(2), 407–416, doi:10.1016/j.atmosenv.2006.07.033, 2007.

Wang, G., Kawamura, K., Xie, M., Hu, S., Gao, S., Cao, J., An, Z. and Wang, Z.: Size-distributions of n-alkanes, PAHs and hopanes and their sources in the urban, mountain and marine atmospheres over East Asia, Atmos. Chem. Phys., 9(22), 8869–8882, 2009a.

Wang, G., Kawamura, K., Xie, M. J., Hu, S. Y., Cao, J. J., An, Z. S., Waston, J. G. and Chow, J. C.: Organic Molecular Compositions and Size Distributions of Chinese Summer and Autumn Aerosols from Nanjing: Characteristic Haze Event Caused by Wheat Straw Burning, Environ. Sci. Technol., 43(17), 6493–6499, doi:10.1021/es803086g, 2009b.

Wang, G., Xie, M., Hu, S., Gao, S., Tachibana, E. and Kawamura, K.: Dicarboxylic acids, metals and isotopic compositions of C and N in atmospheric aerosols from inland China: implications for dust and coal burning emission and secondary aerosol formation, Atmos. Chem. Phys., 10(13), 6087–6096, doi:10.5194/acp-10-6087-2010, 2010.

Wang, G., Chen, C., Li, J., Zhou, B., Xie, M., Hu, S., Kawamura, K. and Chen, Y.: Molecular composition and size distribution of sugars, sugar-alcohols and carboxylic acids in airborne particles during a severe urban haze event caused by wheat straw burning, Atmos. Environ., doi:10.1016/j.atmosenv.2011.02.045, 2011.

Wang, H. B. and Kawamura, K.: Stable carbon isotopic composition of low-molecular-weight dicarboxylic acids and keto-acids in remote marine aerosols, J. Geophys. Res., [Atmos], 111, D0730, doi:10.1029/2005JD006466, 2006.

Wang, J., Ho, S. S. H., Ma, S., Cao, J., Dai, W., Liu, S., Shen, Z., Huang, R., Wang, G. and Han, Y.: Characterization of PM 2.5 in Guangzhou, China: Uses of organic markers for supporting source apportionment, Sci. Total Environ., doi:10.1016/j.scitotenv.2016.01.138, 2016.

Wang, J., Nie, W., Cheng, Y., Shen, Y., Chi, X., Wang, J., Huang, X., Xie, Y., Sun, P., Xu, Z., Qi, X., Su, H. and Ding, A.: Light absorption of brown carbon in eastern China based on 3-year multi-wavelength aerosol optical property observations and an improved absorption Ångström exponent segregation method, Atmos. Chem. Phys., doi:10.5194/acp-18-9061-2018, 2018.

Wang, Y., Zhuang, G., Tang, A., Yuan, H., Sun, Y., Chen, S. and Zheng, A.: The ion chemistry and the source of $PM_{2.5}$ aerosol in Beijing, Atmos. Environ., doi:10.1016/j.atmosenv.2005.03.013, 2005.

Wang, Y. L., Liu, X. Y., Song, W., Yang, W., Han, B., Dou, X. Y., Zhao, X. D., Song, Z. L., Liu, C. Q. and Bai, Z. P.: Source appointment of nitrogen in $PM_{2.5}$ based on bulk $\delta^{15}N$ signatures and a Bayesian isotope mixing model, Tellus, Ser. B Chem. Phys. Meteorol., doi:10.1080/16000889.2017.1299672, 2017.

Widory, D.: Nitrogen isotopes: Tracers of origin and processes affecting PM10 in the atmosphere of Paris, Atmos. Environ., doi:10.1016/j.atmosenv.2006.11.009, 2007.

Wu, J., Hou, B., Ke, R. Y., Du, Y. F., Wang, C., Li, X., Cai, J., Chen, T., Teng, M., Liu, J., Wang, J. W. and Liao, H.: Residential fuel choice in rural areas: Field research of two counties of North China, Sustain., doi:10.3390/su9040609, 2017.

Wu, X., Vu, T. V., Shi, Z., Harrison, R. M., Liu, D. and Cen, K.: Characterization and source apportionment of carbonaceous $PM_{2.5}$ particles in China - A review , Atmos. Environ., 189, 187-212, 2018.

Yan, R., Yu, S., Zhang, Q., Li, P., Wang, S., Chen, B. and Liu, W.: A heavy haze episode in Beijing in February of 2014: Characteristics, origins and implications, Atmos. Pollut. Res., doi:10.5094/apr.2015.096, 2015.

Yang, F., Tan, J., Zhao, Q., Du, Z., He, K., Ma, Y., Duan, F., Chen, G. and Zhao, Q.: Characteristics of PM2.5 speciation in representative megacities and across China, Atmos. Chem. Phys., doi:10.5194/acp-11-5207-2011, 2011.

Yao, X., Chan, C. K., Fang, M., Cadle, S., Chan, T., Mulawa, P., He, K. and Ye, B.: The water-soluble ionic composition of PM2.5 in Shanghai and Beijing, China, Atmos. Environ., doi:10.1016/S1352-2310(02)00342-4, 2002.

Yu, Q., Yang, W., Zhu, M., Gao, B., Li, S., Li, G., Fang, H., Zhou, H., Zhang, H., Wu, Z., Song, W., Tan, J., Zhang, Y., Bi, X., Chen, L. and Wang, X.: Ambient PM2.5 -bound polycyclic aromatic hydrocarbons (PAHs) in rural Beijing: Unabated with enhanced temporary emission control during the 2014 APEC summit and largely aggravated after the start of wintertime heating, Environ. Pollut., doi:10.1016/j.envpol.2018.03.079, 2018.

Yunker, M. B., Macdonald, R. W., Vingarzan, R., Mitchell, R. H., Goyette, D. and Sylvestre, S.: PAHs in the Fraser River basin: a critical appraisal of PAH ratios as indicators of PAH source and composition, Org. Geochem., 33(4), 489–515, 2002.

Zhang, Q., Meng, J., Quan, J., Gao, Y., Zhao, D., Chen, P. and He, H.: Impact of aerosol composition on cloud condensation nuclei activity, Atmos. Chem. Phys., doi:10.5194/acp-12-3783-2012, 2012a.

Zhang, H., Wang, S., Hao, J., Wan, L., Jiang, J., Zhang, M., Mestl, H. E. S., Alnes, L. W. H., Aunan, K. and Mellouki, A. W.: Chemical and size characterization of particles emitted from the burning of coal and wood in rural households in Guizhou, China, Atmos. Environ., doi:10.1016/j.atmosenv.2012.01.042, 2012b.

Zhang, Y. L., Huang, R. J., El Haddad, I., Ho, K. F., Cao, J. J., Han, Y., Zotter, P., Bozzetti, C., Daellenbach, K. R., Canonaco, F., Slowik, J. G., Salazar, G., Schwikowski, M., Schnelle-Kreis, J., Abbaszade, G., Zimmermann, R., Baltensperger, U., Prévôt, A. S. H. and Szidat, S.: Fossil vs. non-fossil sources of fine carbonaceous aerosols in four Chinese cities during the extreme winter haze episode of 2013, Atmos. Chem. Phys., 15(3), doi:10.5194/acp-15-1299-2015, 2015a.

Zhang, J., Qu, C., Qi, S., Cao, J., Zhan, C., Xing, X., Xiao, Y., Zheng, J. and Xiao, W.: Polycyclic aromatic hydrocarbons (PAHs) in atmospheric dust fall from the industrial corridor in Hubei Province, Central China, Environ. Geochem. Health, doi:10.1007/s10653-014-9647-y, 2015b.

Zhang, X., Hecobian, A., Zheng, M., Frank, N. H. and Weber, R. J.: Biomass burning impact on PM2.5 over the southeastern US during 2007: Integrating chemically speciated FRM filter measurements, MODIS fire counts and PMF analysis, Atmos. Chem. Phys., 10(14), 6839–6853, doi:10.5194/acp-10-6839-2010, 2010.

Zhang, W., Zhang, Y.-L., Fang, C., Yankun, X., Yuanyuan, Z., Mengying, B., Xiaoyan, L. and Lin, Y.-C.: High time-resolved measurement of stable carbon isotope composition in water-soluble organic aerosols: method optimization and a case study during winter haze in eastern China, Atmos. Chem. Phys., 19, 11071–11087, doi:https://doi.org/10.5194/acp-19-11071-2019, 2019.

Zhu, C., Kawamura, K. and Kunwar, B.: Effect of biomass burning over the western North Pacific Rim: wintertime maxima of anhydrosugars in ambient aerosols from Okinawa., Atmos. Chem. Phys., 15, 1959–1973, doi:10.5194/acp-15-1959-2015, 2015.

Table 1. Ambient concentrations of organic compounds (ng m^{-3}) and PM$_{2.5}$, OC, EC, WSOC, and SOC (µg m^{-3}) in the atmospheric aerosol samples from the rural and urban sites in eastern China.

Species	Rural (Dongshan)		Urban (Nanjing)	
	Mean±SD[a]	Range	Mean±SD[a]	Range
PM$_{2.5}$	116±49.8	24.2-249	127±55.4	28.7-283
OC	21.7±10.7	3.48-55.0	21.2±9.45	5.03-52.3
EC	2.58±1.68	0.32-11.5	2.44±1.63	0.56-8.91
WSOC	10.1±4.15	1.97-22.6	10.3±4.23	2.31-23.2
SOC	12.9±7.73	0.54-37.4	11.7±6.21	0.16-29.3
Anhydro-sugar				
Levoglucosan	625±456	51.2-539	519±301	105-1775
PAHs				
Fluoranthene (Flu)	6.18±3.91	0.71-20.7	6.40±4.97	0.88-39.9
Pyrene (Pyr)	5.45±3.96	0.56-22.7	4.91±3.63	0.49-25.6
Benzo[a]anthracene (BaA)	1.51±1.70	0.08-8.89	1.02±0.86	0.10-4.61
Chrysene (Chry)	3.31±2.91	0.21-14.9	2.87±2.15	0.31-11.5
Benzo[b,k]fluoranthene (Bb,kF)	5.13±4.06	0.34-21.8	4.31±3.10	0.62-13.4
Benzo[e]pyrene (BeP)	2.55±2.16	0.15-11.6	2.18±1.52	0.04-9.15
Benzo[a]pyrene (BaP)	2.04±2.24	0.09-11.5	1.92±1.44	0.25-6.93
Perylene (Per)	0.40±0.40	0.00-1.85	0.31±0.42	0.00-2.61
Indeno[1,2,3-cd]pyrene (InP)	1.01±0.93	0.06-5.49	1.21±2.45	0.15-24.1
Benzo[ghi]perylene (BghiP)	2.05±1.92	0.10-12.2	2.05±1.94	0.32-13.9
Dibenzo[a,h]anthracene (DahA)	0.18±0.46	0.00-4.55	0.15±0.16	0.00-0.88
Coronene	2.02±1.71	0.00-8.72	1.07±1.50	0.00-12.5
Retene	0.78±1.44	0.00-13.4	0.32±0.52	0.00-3.34
subtotal	32.6±24.7	2.39-136	28.7±20.1	3.54-123
Hopanes				
17α(H)-21β(H)-29-norhopane (C$_{29}$αβ)	0.85±0.71	0.06-2.91	0.60±0.66	0.00-3.70
17α(H)-21β(H)-hopane (C$_{30}$αβ)	0.97±0.79	0.07-3.68	0.66±0.70	0.00-3.99
subtotal	1.83±1.51	0.14-6.42	1.26±1.34	0.00-7.69
***n*-Alkanes**				
C$_{20}$	38.7±28.4	3.34-106	16.9±18.0	1.66-107
C$_{21}$	43.1±33.3	3.94-133	23.5±219.2	4.13-120
C$_{22}$	39.6±928	4.53-147	22.0±17.1	3.97-86.0
C$_{23}$	29.6±120	3.28-93.0	19.0±14.4	2.92-73.0
C$_{24}$	30.4±21.6	3.82-109	19.0±16.9	2.52-89.0
C$_{25}$	27.0±21.7	3.26-148	16.2±12.7	2.63-65.3
C$_{26}$	22.5±17.4	1.48-114	11.4±10.2	0.00-48.5
C$_{27}$	14.4±11.2	1.52-73.3	9.19±7.90	0.00-40.8
C$_{28}$	17.2±12.7	0.25-64.5	8.06±7.27	0.00-35.5
C$_{29}$	15.3±11.9	1.10-63.2	8.14±6.11	0.00-29.1
C$_{30}$	8.71±6.69	0.19-30.0	4.24±4.57	0.00-29.8
C$_{31}$	7.69±5.29	0.27-26.4	6.63±6.23	0.00-26.7
C$_{32}$	4.04±2.87	0.00-14.4	1.94±2.30	0.00-12.2
C$_{33}$	4.37±4.22	0.00-21.3	2.73±3.37	2.7312.9
subtotal	302±206	36.3-943	169±131	34.2-575

[a]Standard deviation (OC refers to organic carbon, EC refers to elemental carbon, WSOC refers to water-soluble organic carbon and SOC refers to secondary organic carbon.)

41

Table 2. The values of inorganic components (µg m^{-3}) and $\delta^{13}C$ of TC and $\delta^{15}N$ of TN (%) in the rural and urban samples (PM$_{2.5}$) in the YRD region in winter.

Species	Rural		Urban	
	Mean±SD[a]	Range	Mean±SD[a]	Range
Na$^+$	0.49±0.23	0.10-1.25	0.62±0.33	0.18-1.91
NH$_4^+$	16.8±7.53	3.89-36.0	20.9±11.1	4.77-45.8
K$^+$	1.0±0.52	0.12-2.37	1.32±0.66	0.29-3.81
Mg^{2+}	0.06±0.08	0.00-0.43	0.15±0.13	0.00-0.68
Ca^{2+}	1.41±3.11	0.01-16.9	2.88±3.53	0.15-16.2
Cl$^-$	4.24±3.24	0.30-15.5	6.15±4.82	0.77-21.1
NO$_2^-$	0.03±0.04	0.00-0.27	0.12±0.11	0.00-0.72
NO$_3^-$	28.4±15.5	3.57-67.7	30.7±16.9	3.13-71.2
SO$_4^{2-}$	23.5±9.84	6.61-47.1	25.7±14.2	7.13-76.1
$\delta^{13}C$ (%)	-25.3±0.80	-22.7 to -26.6	-25.3±1.05	-22.2 to -27.4
$\delta^{15}N$ (%)	+0.87±5.02	-9.59 to +13.7	+1.50±4.30	-6.24 to +11.6

Table 3. The values of different chemical species in the rural and urban samples (PM$_{2.5}$) from eastern China during the haze, dust, and clear day events.

| Species	Rural			Urban		
	Haze	Dust	Clear	Haze	Dust	Clear
[a]PM$_{2.5}$	144±40.0	120±38.8	56.7±22.6	156±49.2	115±39.9	66.6±20.3
[a]OC	25.7±10.3	24.7±7.36	10.5±5.22	24.1±8.94	23.9±7.57	10.6±4.50
[a]EC	2.60±1.14	4.03±2.44	1.33±0.82	2.27±1.12	3.70±1.90	1.08±0.44
[a]WSOC	12.0±3.45	10.8±3.11	5.39±2.31	11.3±3.38	11.1±3.65	5.97±3.74
[a]SOC	16.9±7.09	11.0±6.69	6.03±3.56	15.3±5.65	9.45±5.26	6.41±3.28
[b]Levoglucosan	778±493	597±425	349±237	633±306	526±246	238±114
[b]PAHs	41.4±28.7	30.0±9.18	15.0±16.6	36.7±22.5	25.6±12.8	12.6±5.66
[b]Hopanes	2.24±1.60	1.86±0.88	0.67±1.06	1.82±1.62	0.83±0.63	0.45±0.16
[b]n-alkanes	334±213	394±133	122±105	241±135	115±83.1	63.2±26.5
[a]Ca^{2+}	0.39±0.46	5.36±5.19	0.38±0.47	1.50±1.71	6.70±4.08	1.09±0.55
[a]NH$_4^+$	22.4±5.15	12.9±6.20	9.07±3.29	29.0±8.34	12.9±7.73	12.9±4.10
[a]NO$_3^-$	36.9±12.7	29.8±13.7	10.6±6.47	41.5±15.1	23.9±11.2	13.0±5.47
[a]SO$_4^{2-}$	30.0±8.10	20.1±7.29	14.0±4.72	34.4±14.0	16.9±7.90	16.2±4.42
$\delta^{13}C$ (%)	-25.5±0.67	-24.5±0.72	-25.5±0.71	-25.5±0.97	-25.1±1.25	-25.7±0.73
$\delta^{15}N$ (%)	-0.77±3.44	+6.22±5.61	-0.79±3.92	+0.64±3.62	+5.63±3.06	-1.04±3.02

[a]µg m^{-3}, [b]ng m^{-3}
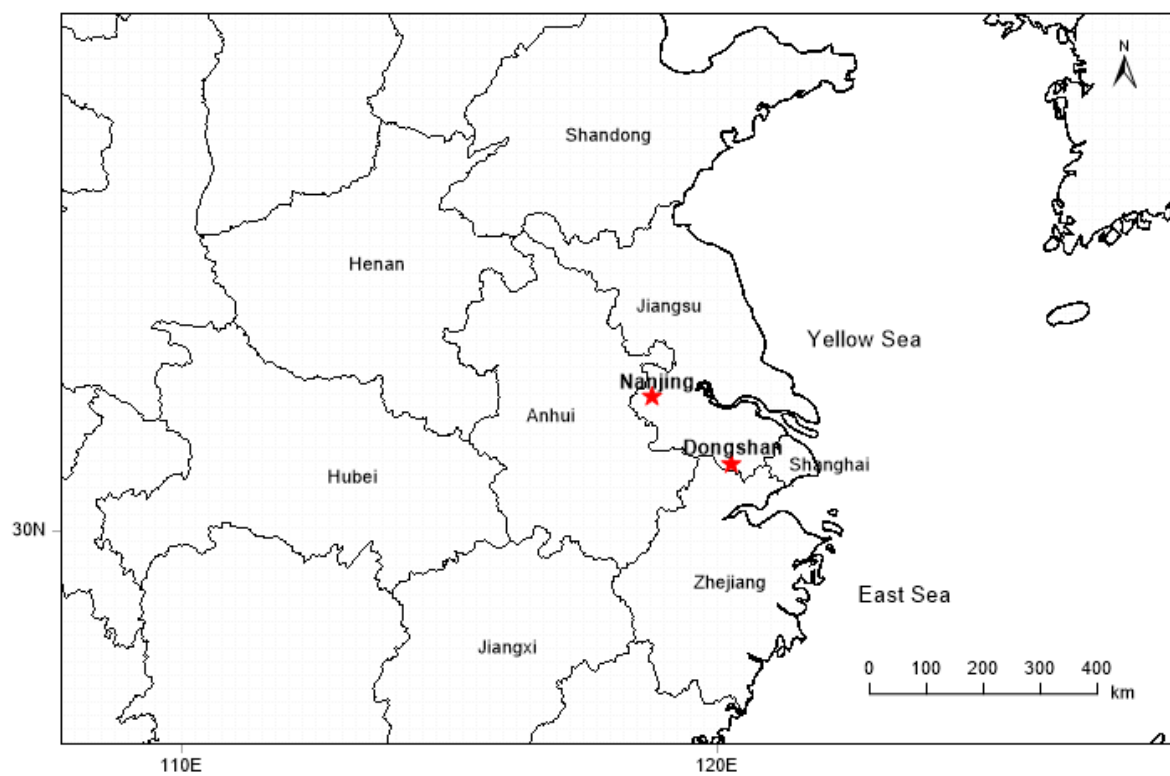
Figure 1. A map of sampling sites in the rural (Dongshan) and urban (Nanjing) area located in eastern China.
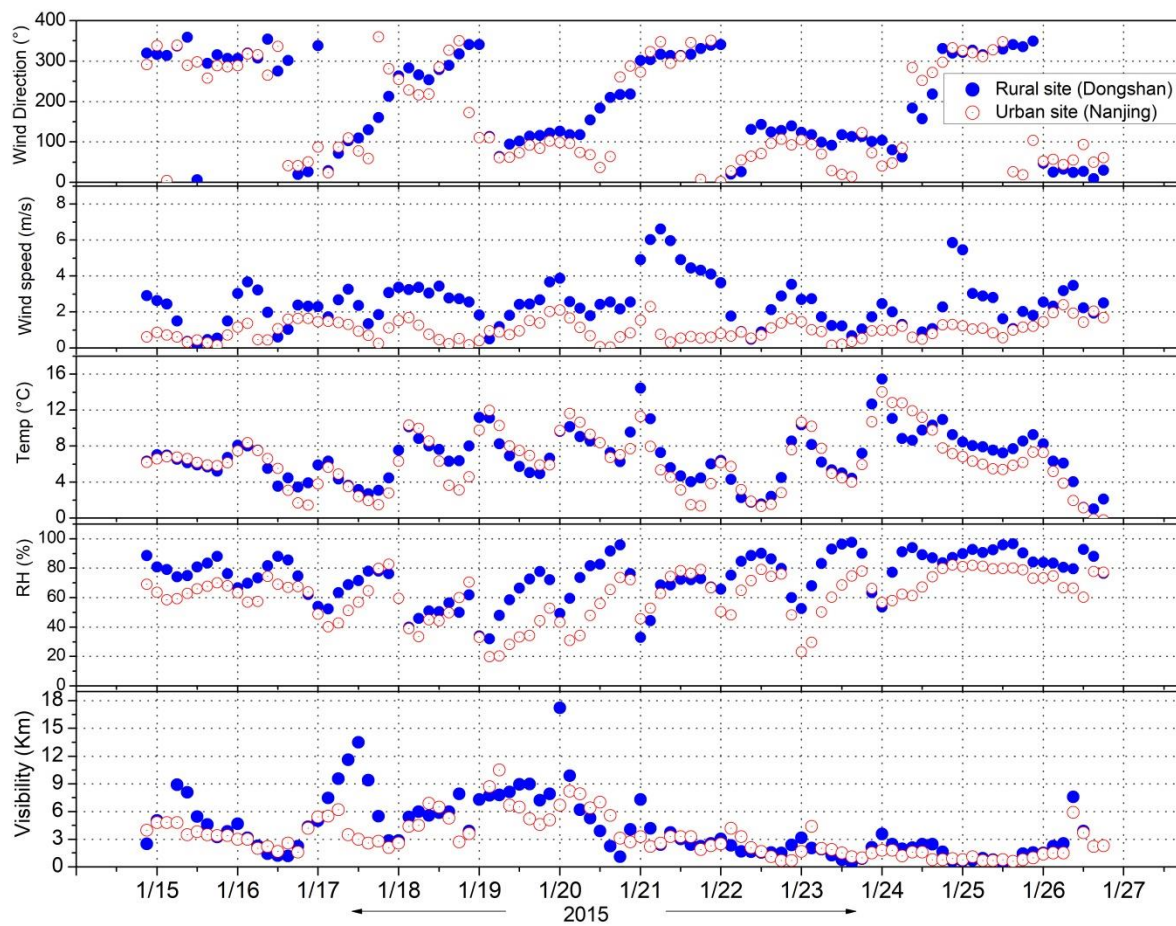
Figure 2. Diurnal variations of wind direction, wind speed, temperature, relative humidity (RH%) and visibility in the rural and urban aerosols from 15-27 January 2015.
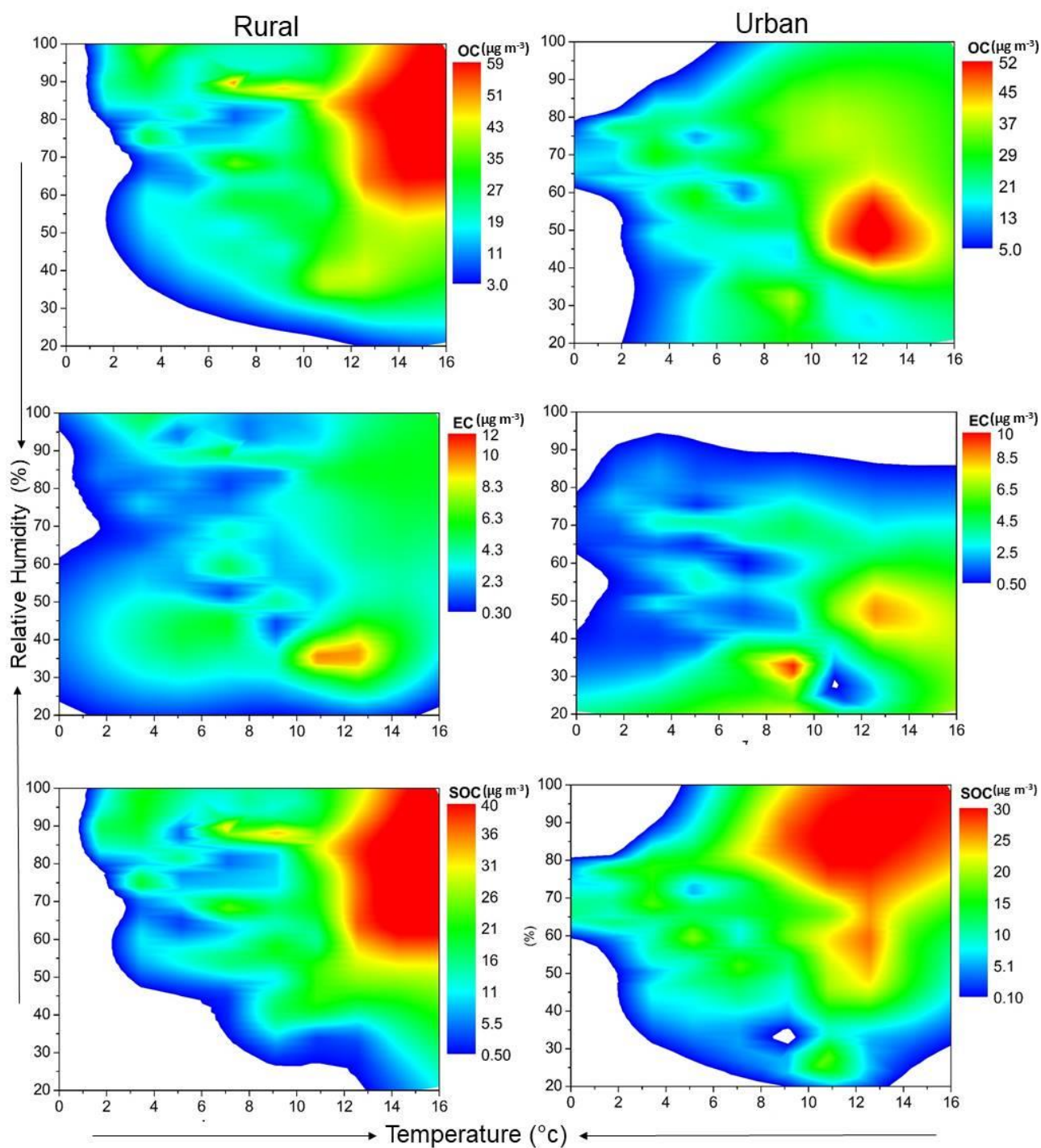
Figure 3. Distribution of OC, EC, and SOC mass concentrations in the rural and urban aerosols from 15-27 January 2015. The color scale reflects mass concentrations.
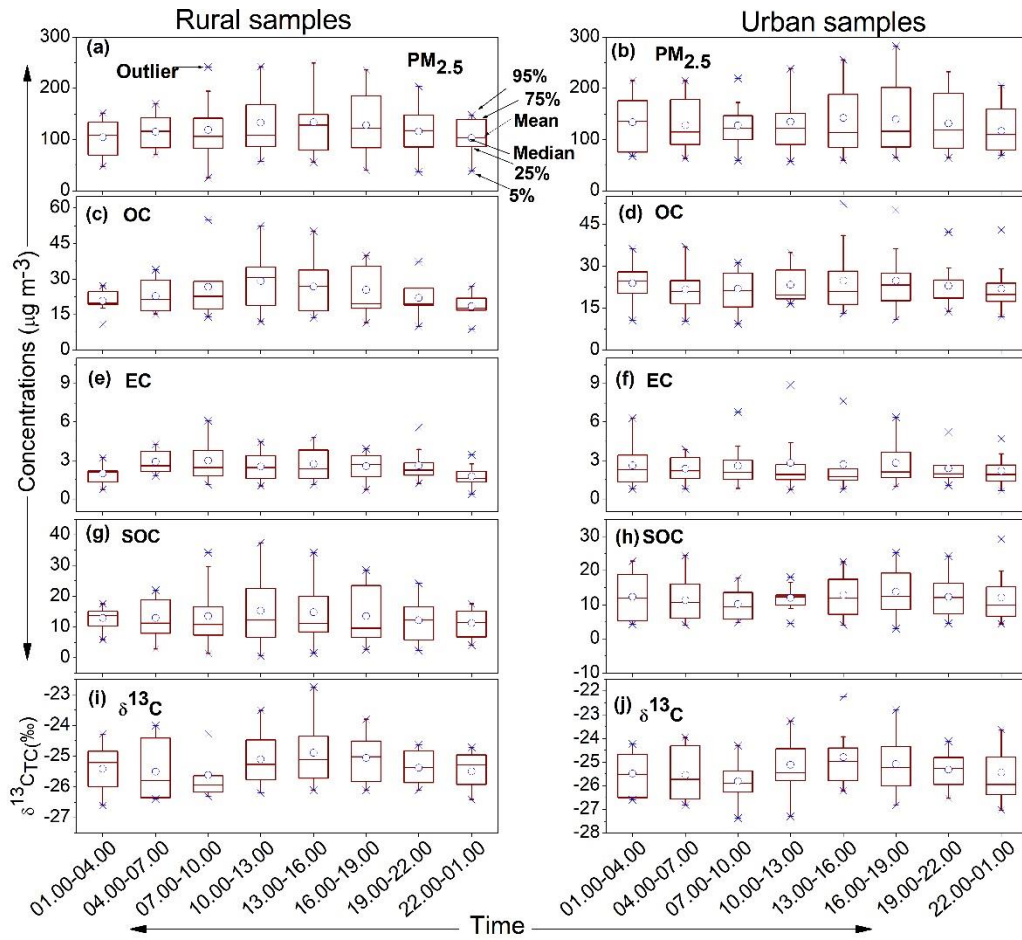
45

Figure 4. Diurnal variations of the values of PM$_{2.5}$, OC, EC, SOC, and δ^{13}C at the rural and urban samples in the YRD region. The mean, median, 5th, 25th, 75th, and 95th percentiles are indicated in the first left figure of the top row.
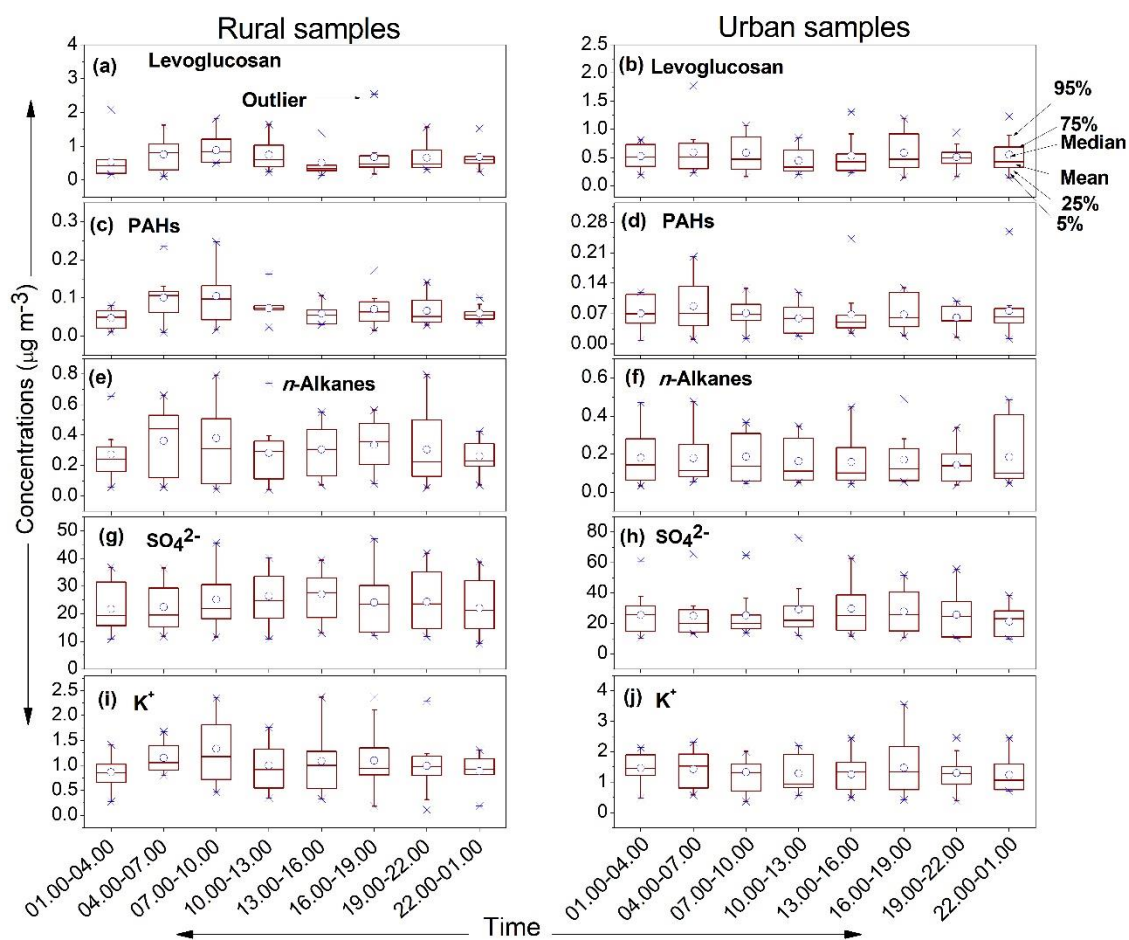
Figure 5. Diurnal variations of the concentrations of different chemical species at the rural and urban samples in the YRD region. The mean, median, 5th, 25th, 75th, and 95th percentiles are indicated in the first right figure of the top row.

47
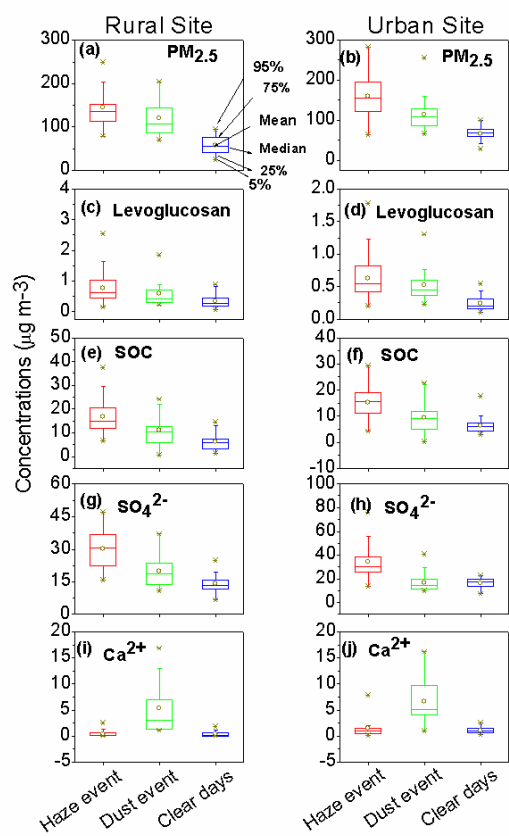
Figure 6. Concentrations of chemical species (μg m^{-3}) in the rural and urban areas from 15-27 January 2015. The mean, median, 5th, 25th, 75th, and 95th percentiles are indicated in the first figure of the top row.
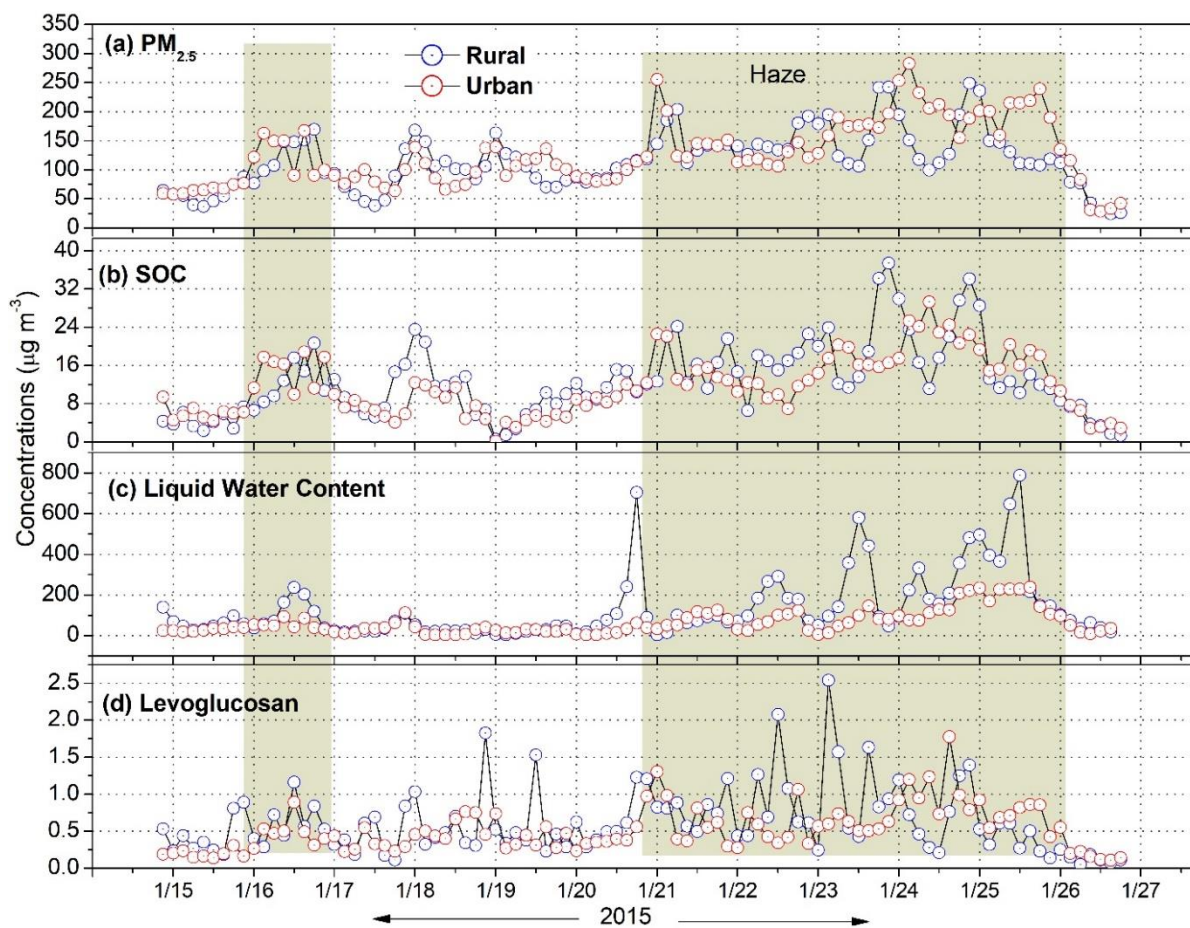
Figure 7. Three hours variations of (a) $PM_{2.5}$, (b) secondary organic carbon (SOC), (c) liquid water content and (d) levoglucosan mass concentrations during our study period.
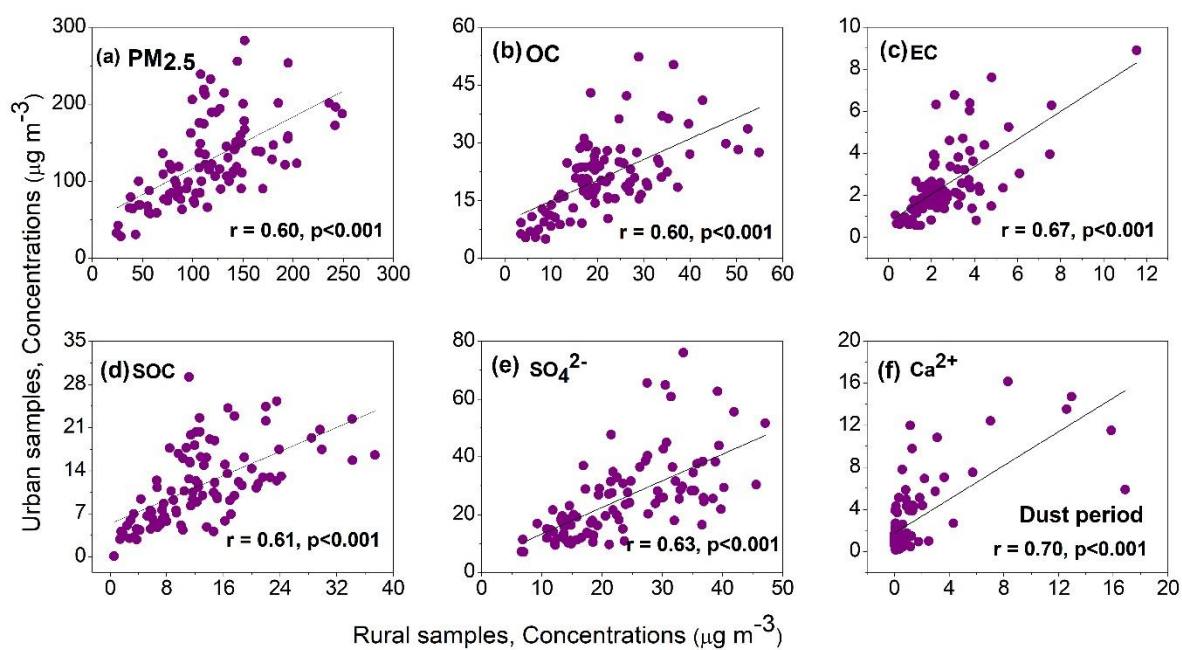
Figure 8. Correlations of different species between rural and urban samples during the sampling period in the YRD region, China.
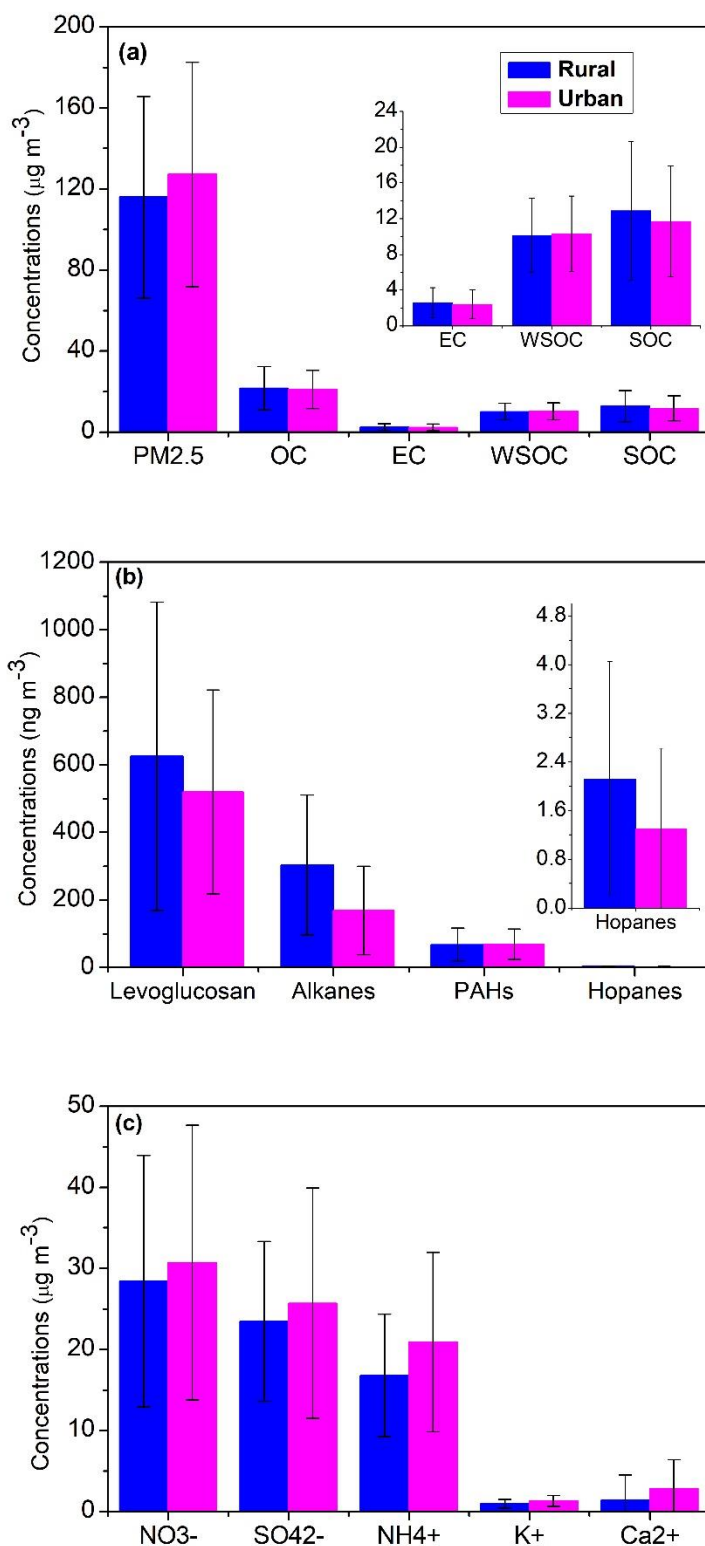
Figure 9. Concentrations of (a) PM$_{2.5}$, OC, EC, WSOC, and SOC (b) organic compound classes (c) inorganic components detected in the rural and urban aerosols. PAHs refers to polycyclic aromatic hydrocarbons. The inset panels represent the corresponding components for which the concentrations are low.
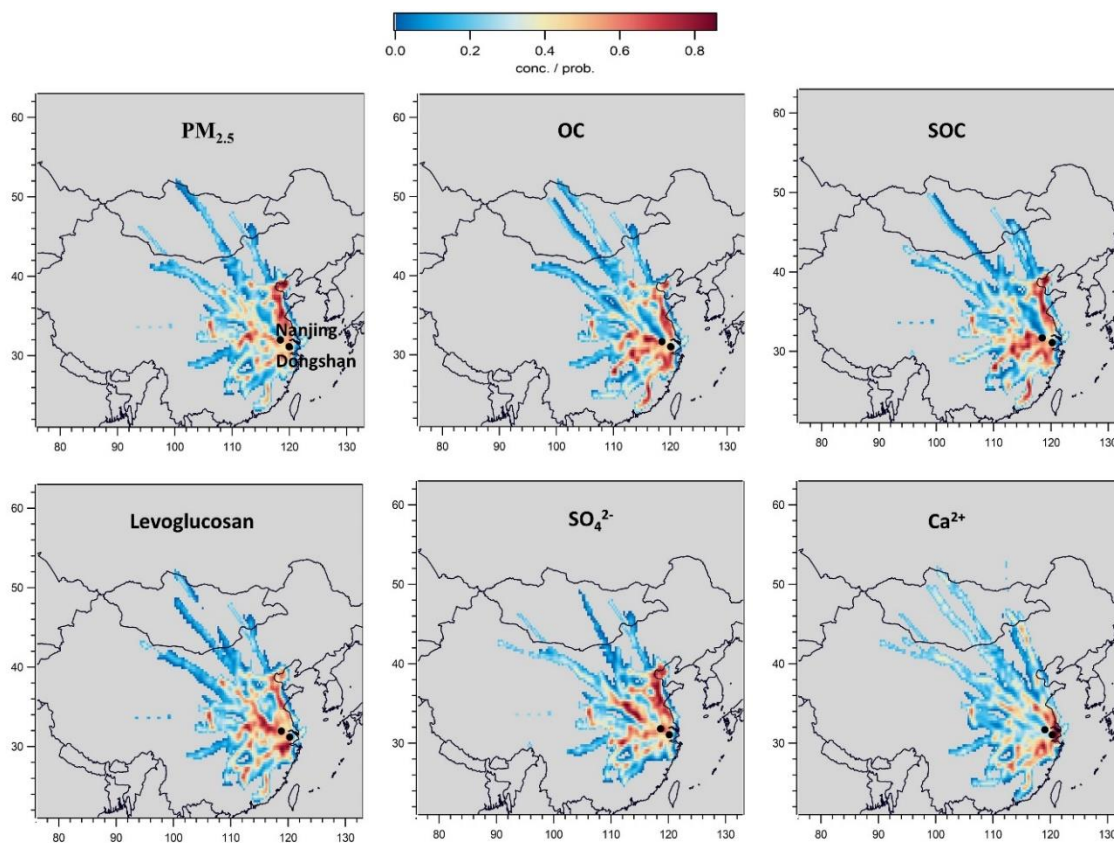
Figure 10. The potential source contribution function (PSCF) of $PM_{2.5}$, OC, SOC, levoglucosan, SO_4^{2-}, and Ca^{2+} at the rural site in eastern China during the sampling period. The color scales indicate the values of PSCF.
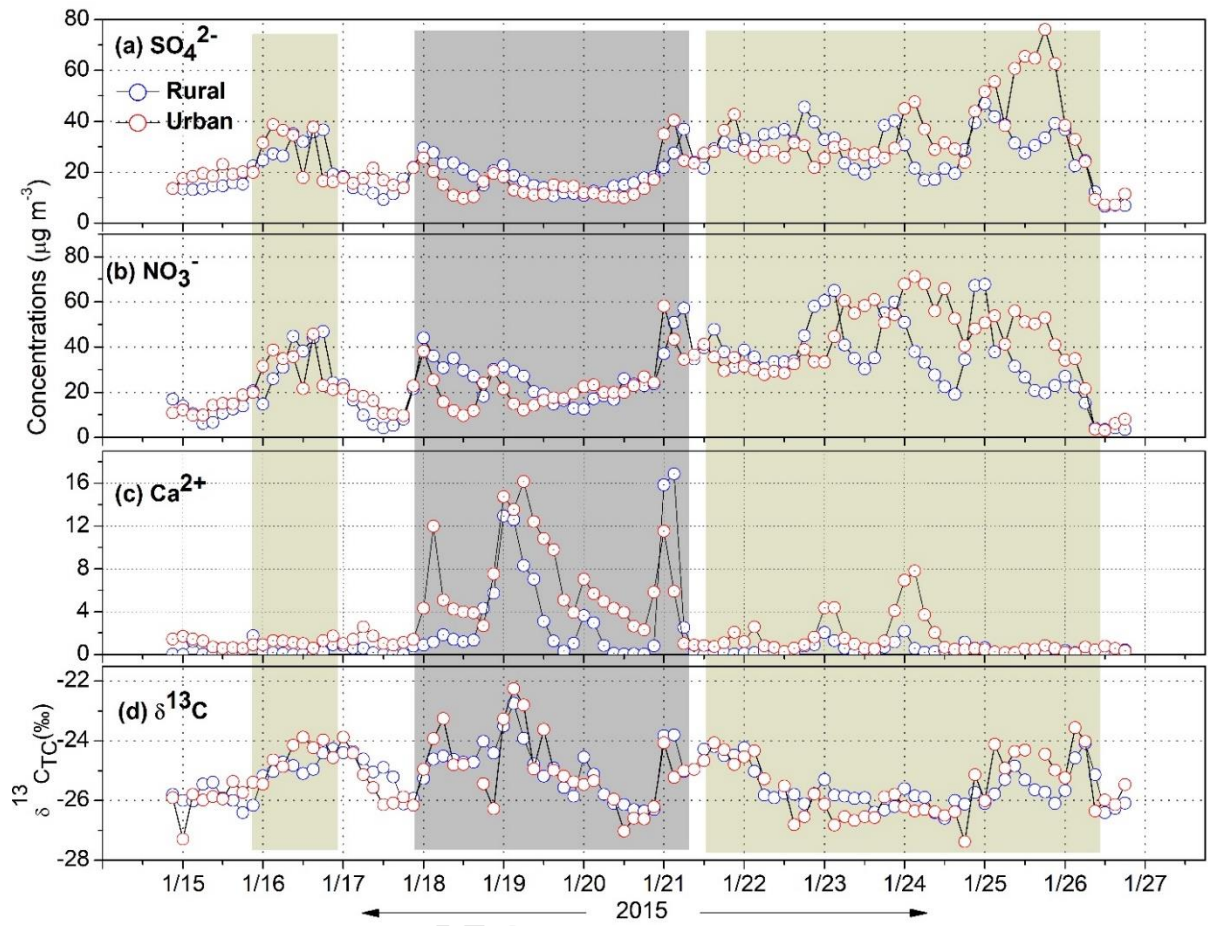
Figure 11. Time series of the concentrations of inorganic ions and $\delta^{13}C$ of TC at the rural and urban samples during the study period in the YRD region.

Conflict of Interest Statement
We all authors declare that we have no conflict of interest.

Author Statement

Md. Mozammel Haque: Data analysis and Writing- Original draft preparation. **Cao Fang**: Project administration and Organized Campaign. **Jürgen Schnelle-Kreis**: Investigation, Reviewing and Editing. **Gülcin Abbaszade**: Chemical analysis of organic compounds. **Xiaoyan Liu**: Analysis of carbonaceous components and major ions, **Mengying Bao**: Collected aerosol samples. **Wenqi Zhang**: Collected aerosol samples. **Yan-Lin Zhang**: Supervision.
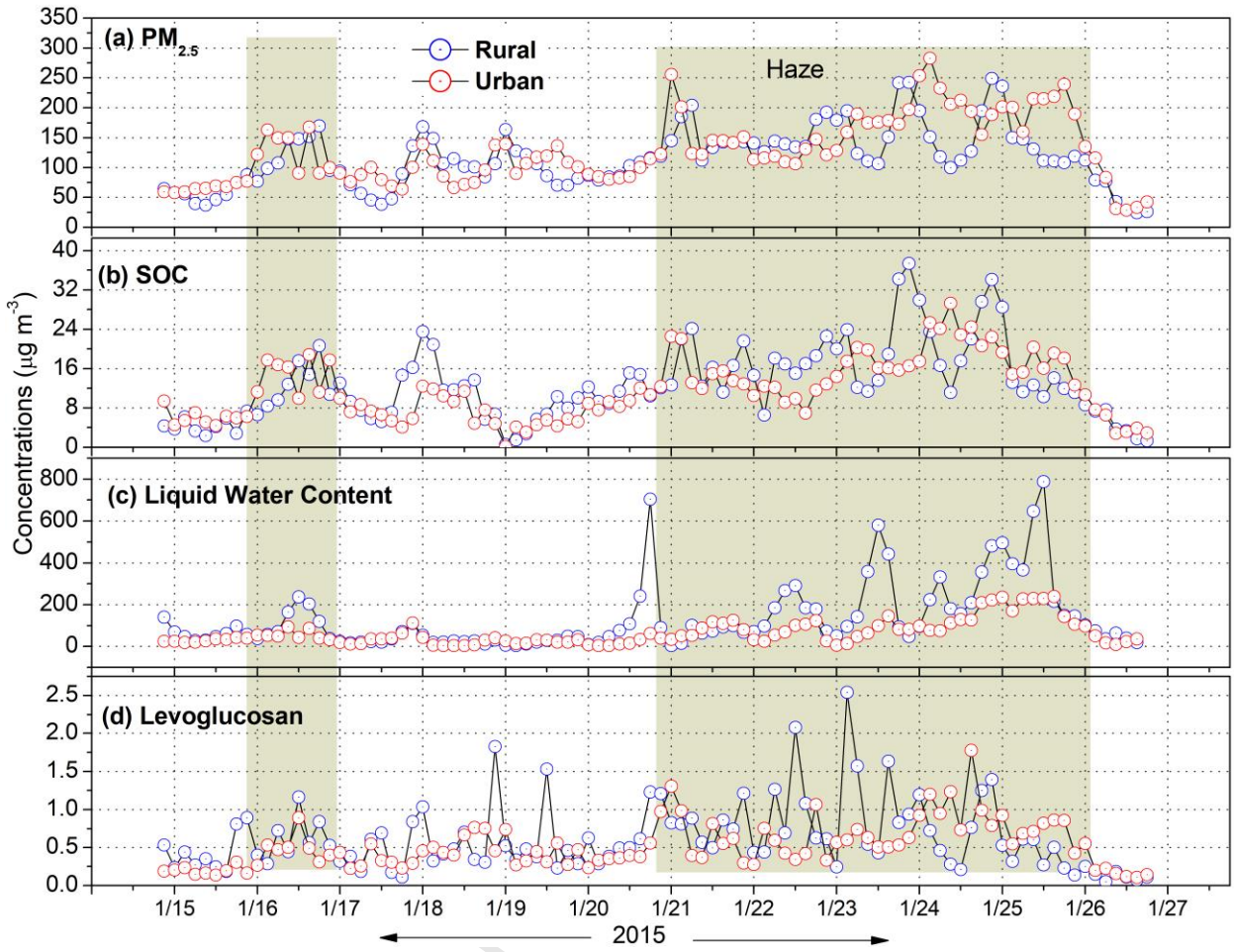
Graphical abstract

Highlights

● Meteorological factors such as relative humidity, temperature and solar radiation, etc., play an important role to form a secondary aerosol during haze period, which enhances the pollution level in eastern china.

● Molecular compositions of aerosols for both sampling sites reflecting their similar pollution sources and/or formation process.

● Anthropogenic sources such as fossil fuel combustion and biomass burning emissions significantly contribute to $PM_{2.5}$ in the YRD region atmosphere.

● Local sources and regional transport increase the atmospheric pollutions in the YRD region.